Dalton Transactions

Synthetic pathways for the preparation of the BODIPY analogues: aza-BODIPYs, BOPHYs and some other pyrrole-based acyclic chromophores

Journal:	*Dalton Transactions*
Manuscript ID	DT-PER-11-2020-003964.R1
Article Type:	Perspective
Date Submitted by the Author:	17-Dec-2020
Complete List of Authors:	Shamova, Liliya ; University of Manitoba, Chemistry Zatsikha, Yuriy; University of Manitoba, Chemistry Nemykin, Viktor; The University of Tennessee Knoxville, Chemistry

Synthetic pathways for the preparation of the BODIPY analogues: aza-BODIPYs, BOPHYs and some other pyrrole-based acyclic chromophores

Liliya I. Shamova,[a] Yuriy V. Zatsikha,[a] and Victor N. Nemykin*[a,b]

[a] *Department of Chemistry, University of Manitoba, Winnipeg, MB R3T 2N2, Canada*
[b] *Department of Chemistry, University of Tennessee, Knoxville, TN 37996, USA*

Abstract

This mini-review summarizes the synthetic strategies for the preparation and post functionalization of aza-BODIPYs, BOPHYs, "half-Pcs", biliazines, MB-DIPYs, semihemiporphyrazines, BOIMPYs, BOPPYs, BOPYPYs, BOAHYs, and BOAPYs.

1. Introduction

Porphyrins and their natural structural analogues are well-known "pigments" of life that are responsible for a variety of biological functions ranging from the oxygen carrier to the light-harvesting in plants and bacteria.[1-4] There fascinating aromatic macrocycles along with their synthetic structural analogues such as phthalocyanines[5-7] and tetraazaporphyrins[8-10] were intensively studied over the last century for traditional as well as new, high-tech applications. Although known for several decades, the alicyclic analogues of the porphyrins (i.e. 4,4-difluoro-4-bora-3a,4a-diaza-s-indacenes, BODIPYs),[11-17] tetraazaporphyrins (aza-BODIPYs), [18-21] and phthalocyanines (benzo-fused aza-BODIPYs)[22] received much less attention, predominantly because of their lower stability toward acids, bases, and oxidants. Fortunately, during the last several decades, these bright chromophores attracted a lot of well-deserved scientific interest because their optical, fluorescence, and redox properties, in many cases, can be tuned much easier than those in traditional porphyrins and their analogues. Not surprisingly, in the pursuit of further structural modifications, several research groups reported recently quite an array of interesting BODIPY and aza-BODIPY analogues. Although many reviews that target specific properties and applications of the BODIPYs are now available, aza-BODIPYs and especially their structural analogues were not overviewed to a large extent. Thus, in this mini-review, we will summarize the synthetic strategies for the preparation and post functionalization of the large array of chromophores such as aza-BODIPYs, BOPHYs, "half-Pcs", biliazines, MB-DIPYs,

semihemiporphyrazines, BOIMPYs, BOPPYs, BOPYPYs, BOAHYs, and BOAPYs. In general, these systems are limited to three motifs shown in Chart 1. Many of these systems were discovered during the last decade and remain unexplored to a large extent. Taking into consideration limited scope of this perspective, the other related systems such as dipyridylisoindoles, dipyridyl methylenes and methanes, and pyrrole-pyridine boron fluorophores will not be discussed.

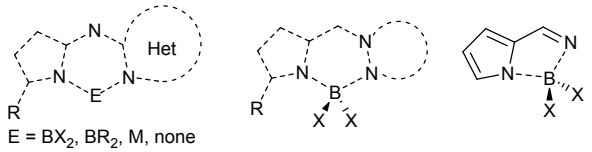

Chart 1.

2. Aza-BODIPYs

2.1. Direct synthesis. Azadipyrromethenes (aza-DIPYs) and respective boron compounds (aza-BODIPYs) are direct analogues of the BODIPYs in which carbon *meso*-atom is replaced with the nitrogen one. Although they were discovered back in 1943 by Davies and Rogers[23], the convenient methods for the preparation of these compounds were first developed by O'Shea's group only 60 years later. Among several available general methods, one of the most popular approaches for the synthesis of tetraaryl-substituted azadipyrromethene scaffold **3** relies on the simple chalcone chemistry[24]. In this synthetic strategy, readily available (via aldol condensation of corresponding benzaldehydes and acetophenones) chalcones **1** (chalcones with both $Ar_1 = Ar_2$ or $Ar_1 \neq Ar_2$ pattern can be used) are introduced in the 1,4-Michael addition of nitromethane to form the key intermediates **2** (Scheme 1). Further condensation of these nitrobutanone derivatives **2** in refluxed alcohol in the presence of an ammonium source results in the formation of a crude azadipyrromethene (aza-DIPY) **3** which precipitates from the solvent and can be easily collected by filtration or purified by chromatography. The aza-DIPYs **3** can be used for the preparation of a large variety of the transition-metal and main-group complexes.[22] In addition, the most popular boron derivatives **4** (aza-BODIPYs) can be synthesized from **3** and boron trifluoride etherate in the presence of a base.

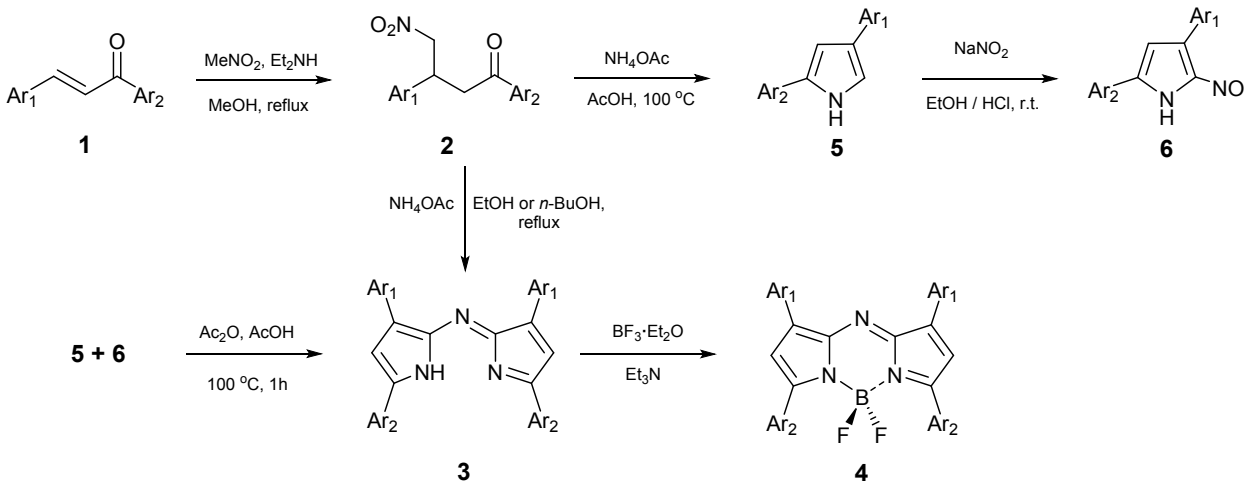

Scheme 1.

To accommodate the needs for the introduction of the different functional groups, the asymmetric approach synthetic strategy was introduced by the same group in 2005[25]. In this approach, 2,4-diarylpyrrole **5** is synthesized first from the same 4-nitroso-1,3-diarylbutan-1-ones **2** used in the previous method. The 2,4-diarylpyrroles **5** were then introduced in the room-temperature reaction with sodium nitrite to form the nitrosopyrroles **6**. Cross-condensation of the pyrroles **5** and nitrosopyrroles **6** under elevated temperature in acetic acid leads to the formation of aza-DIPYs **3**, which can be transformed in the boron derivatives **4**. If nitrosopyrrole **6** reacts with the independently prepared 2,4-diarylpyrrole **5** (say, carrying Ar_3 and Ar_4 substituents), then up to four different aryl groups can be introduced in the aza-DIPY core.[22] Aryl groups (Ar_1 and Ar_2, Scheme 1) can carry a wide variety of substituents such as halogens, esters, amines, and anilines.

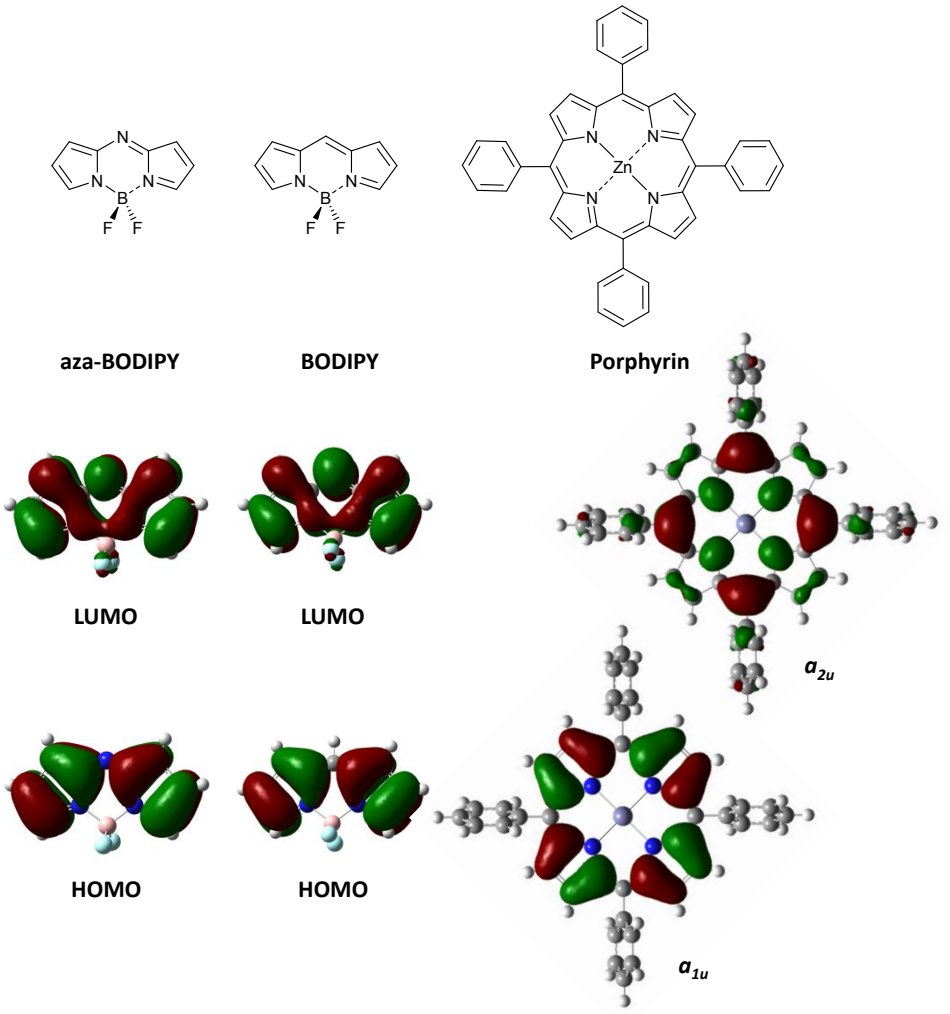

Figure 1. Typical HOMO and LUMO of BODIPY/aza-BODIPY in comparison with the Gouterman's a_{1u} and a_{2u} orbitals.

Unless altered by the specific substituents (for instance ferrocene groups), the electronic structure of the aza-BODIPYs resembles that of BODIPYs. In particular, the HOMO of the typical aza-BODIPY resembles a half of the well-known Gouterman's a_{1u} orbital of the porphyrin, which has most of its electron density located at the pyrrolic α- and β-carbons (Figure 1). The LUMO of the typical aza-BODIPYs resembles the well-known Gouterman's a_{2u} orbital of the porphyrin, which has significant electron density at the pyrrolic nitrogen atoms and the *meso*-atom. Since the BODIPY's *meso*-carbon atom in the aza-BODIPYs is replaced with more electronegative nitrogen atom, the LUMO in aza-BODIPYs is significantly stabilized compared to that in BODIPYs (unless BODIPYs are modified with the electron-withdrawing groups at the

meso-position, see, for instance, ref. 26). As a result, the HOMO-LUMO energy gap in the aza-BODIPYs is significantly smaller than that in the BODIPYs, which leads to a large red-shift of the most intense low-energy band in their UV-vis spectra. The introduction of organometallic ferrocene groups to the aza-BODIPY core allows low-energy metal-to-ligand charge-transfer (MLCT) transitions, which were observed between 800 and 1200 nm for the di-[27] and tetraferrocenyl-containing[28] aza-BODIPYs. The bulky groups in the positions 1 and 7 of the aza-BODIPY core are usually poorly conjugated with the chromophore's π-system (see, for instance X-ray structures of 1,7-dipyrene- containing aza-BODIPYs, Figure 2).[29] 1,7-dipyrene-containing aza-BODIPYs are able to form well-ordered co-crystallites with the C_{60} fullerene (Figure 3).[29] Most of the aza-BODIPY derivatives feature small Stokes shifts, high molar extinction coefficients of absorbance, and high quantum yields of emission, as well as narrow absorbance and emission full widths at half maxima (FWHM).

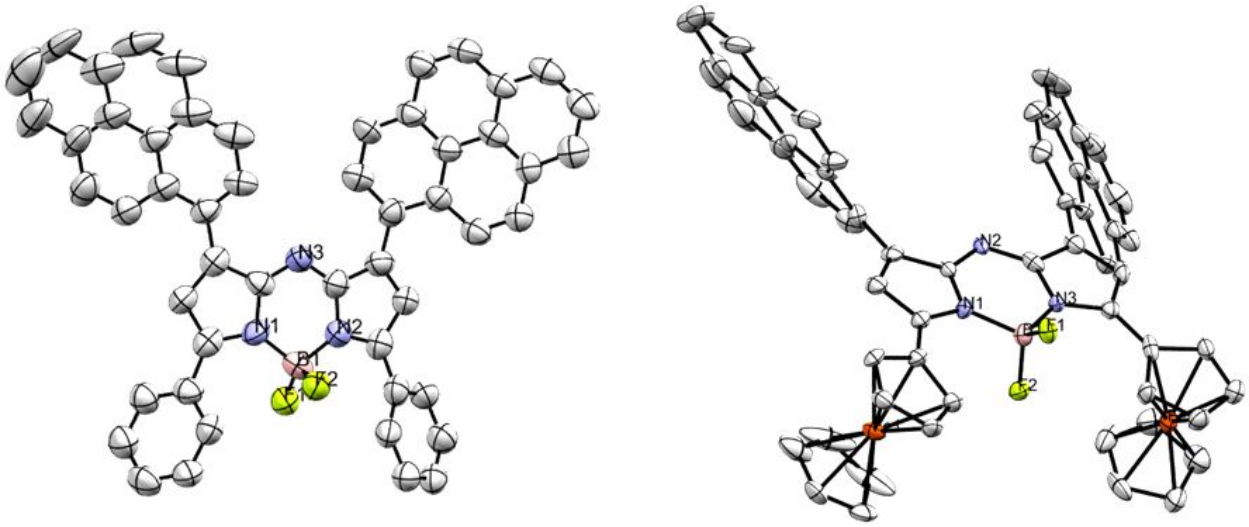

Figure 2. X-ray structures of the 1,7-dipyrene aza-BODIPYs. Adapted from ref. 29 with permission from the American Chemical Society, copyright 2018.

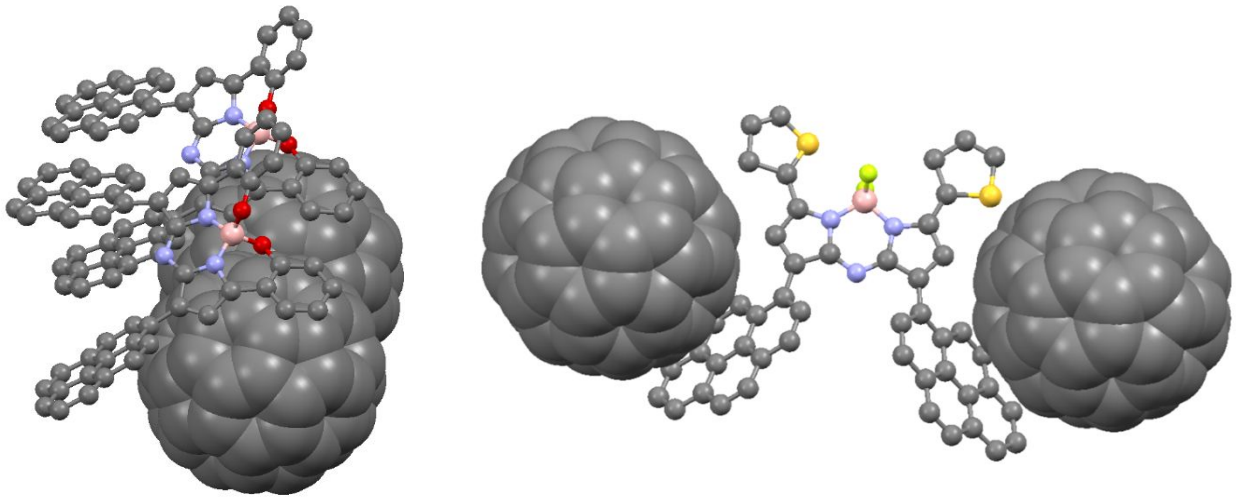

Figure 3. X-ray structures of the 1,7-dipyrene aza-BODIPYs with C_{60} fullerene. Reproduced from ref. 29 with permission from the American Chemical Society, copyright 2018.

2.2. Post-functionalization.

2.2.1. Direct halogenation and sulfonation. O'Shea's and Sauve's groups have reported di-bromination[24] and di-iodination[30] of the pyrrolic positions of the aza-DIPY core **3** at room temperature to form **7** in high yields using Br_2 and *N*-iodosuccinimide, respectively. Di-brominated[31] azadipyrromethene ligands for Au(I) complexes were prepared using *N*-bromosuccinimide. Mono-bromination[32] could be achieved by the use of one equivalent of the brominating agent. Once formed from the aza-DIPYs, the classic tetraaryl aza-BODIPY core is significantly more resistant toward direct halogenation reaction. However, the introduction of the electron-donating groups (i.e. carbazole groups) at the β-pyrrolic positions can allow direct halogenation (for instance iodination) of the aza-BODIPY core with *N*-iodosuccinimide to form aza-BODIPYs **8** (Scheme 2).[33]

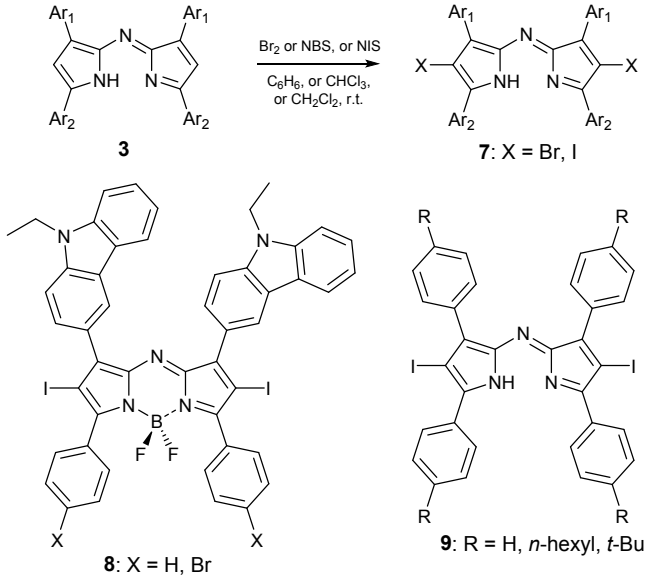

Scheme 2.

Introduction of the halogen atom not only alters the conformation of other substituents at the azadipyrromethene core but also dramatically increases the intersystem crossing ability of the fluorophore due to the heavy atom (spin-orbit coupling) effect. Consequently, halogenated aza-DIPYs and their metal complexes demonstrate excellent single-oxygen production ability and have potential for use as the photosensitizers in anti-bacterial or anti-cancer therapies.[34] Apart from the photosensitizing effect, halogenation suppressed fluorescence quantum yield in tetraphenyl aza-BODIPY;[35] increased Stokes shift and dramatically increased a triplet quantum

yield in diiodinated *N*-ethylcarbazole proximally disubstituted aza-BODIPYs **8** compared to the non-halogenated analogues.[33] The halogenation of β-positions of aza-BODIPY core increases the photostability of resulting difluoroborates under the UV-irradiation as was demonstrated for tetraphenyl aza-BODIPY.[36] Interestingly, aza-BODIPY **9** was found to lose BF_2 fragment in chlorobenzene at 70 ºC.[30] Sulfonation at 2- and 6-positions of aza-DIPY can be achieved by using chlorosulfonic acid in DCM at low temperature. However, the same reaction conducted on aza-BODIPY core led to the loss of BF_2 fragment.[37]

2.2.2. Coupling reactions. 2,6-Dihalogen-substituted tetraarylazadipyrromethenes can be introduced into a variety of coupling reactions. For instance, Sonogashira-Hagihara coupling reaction in chlorobenzene/Et_3N system at 70ºC for 48 h with of tetrakis(triphenylphosphine) palladium(0) and copper(I) iodide as catalysts was used by Sauve's group[30] in 2015 for the preparation of conjugated aza-DIPY oligomers. The same coupling reaction was used by Ng's group[38] in 2018 for the synthesis of aza-BODIPY derivatives substituted with two strong electron-donating 4-(dimethylamino)phenylethynyl (compound **11**, Scheme 3) or 4-(diphenylamino)phenylethynyl groups.

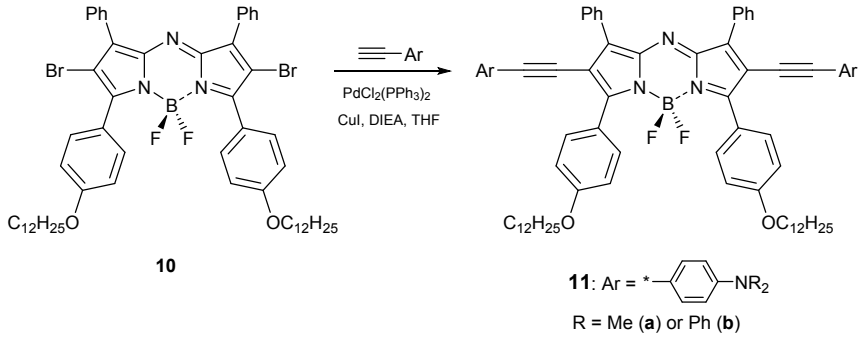

Scheme 3.

To enhance the solubility and, therefore, the yield of the products, dodecyl chains were introduced to aza-BODIPY core **10**. The UV-vis spectrum of aza-BODIPY **11** is extended to the NIR region (up to 830 nm) and clearly reflective of the conjugation of the -C≡C-*p*-C_6H_4-NR_2 fragments to the aza-BODIPY's π-system. Not surprisingly, the protonation at the aminogroup in **11** upon the addition of trifluoroacetic acid results in remarkable spectroscopic changes. Sonogashira coupling reaction was also used recently for the preparation of aza-BODIPY dyes tetrasubstituted by dihexylaminophenylethynyl fragment[39] and for conjugating iodoarylated-aza-BODIPY to estradiol, testosterone, and 19-nortestosterone derivatives with the aim of developing receptor-based fluorescence ligands.[40]

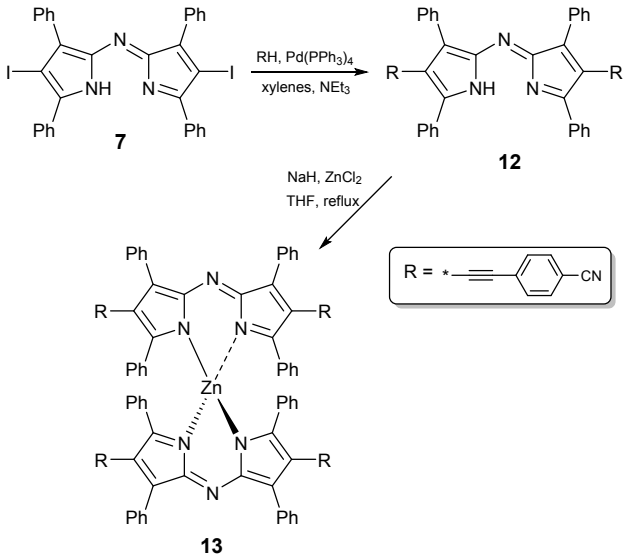

Scheme 4.

In order to create electron-deficient non-fullerene acceptors, the electron-accepting cyano groups were introduced to the extended ligand **12** by Sauve's group (Scheme 4). Compound **12** was prepared via Sonogashira coupling in a good yield and then used to form zinc complex **13**.[41] Interestingly, Stille coupling reaction conditions did not work well for this platform, resulting in a product that contained impurities that could not be easily removed by solvent wash or chromatography.[41]

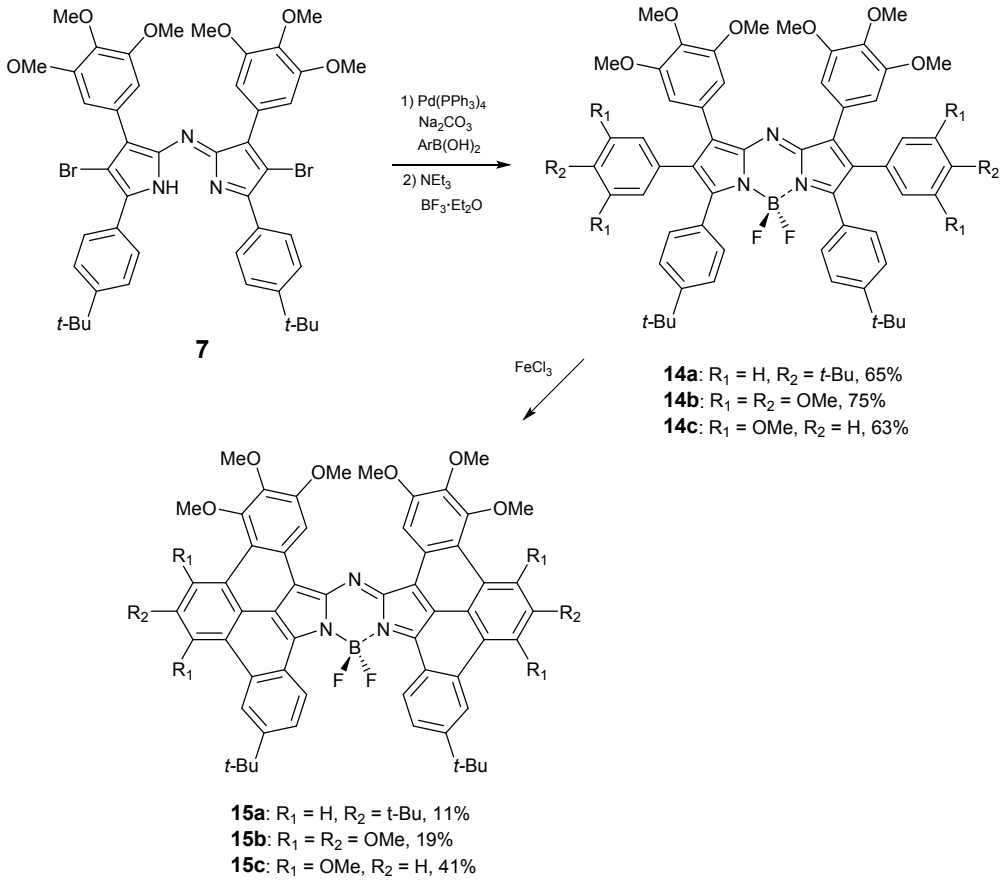

Scheme 5.

2-Bromo-substituent in aza-BODIPY core can be converted to anisyl group using anysilboronic acid under mild, palladium(0)-catalyzed catalysed Suzuki coupling conditions.[42] The same method was used by this group to synthesize a series of 1,2,3,5,6,7-hexaarylated aza-BODIPYs in 25-35% reaction yeilds.[43] Jiao's group has prepared a series of hexaarylated aza-BODIPYs **14a-c** (Scheme 6). These compounds were used for the regioselective oxidative ring fusion reaction in the presence of iron(III) chloride to form a set of the partially annulated β,β-biphenanthrene-fused aza-BODIPYs (96% yield)[44] as well as fully annulated products **15a-c** (11-41% reaction yields).[45] These fluorophores with up to 13 aromatic ring fusions[46] exhibit strong NIR (up to 878 nm) absorption and NIR (up to 907 nm) emission.

2.2.3. Formylation. The synthetic route to β-monoformyl-substituted aza-BODIPYs was established by Jiao[47] and co-workers in 2009. They used a modified Vilsmeier-Haack reaction with Vilsmeier reagent generated *in situ* from DMF and $POCl_3$. A β-formylaza-BODIPY **16** was generated in 86% yield. Introduction of an electron-withdrawing aldehyde group to one β-

position of aza-BODIPY core seems to prevent second electrophilic reaction and yields only mono-substituted product (Scheme 6).

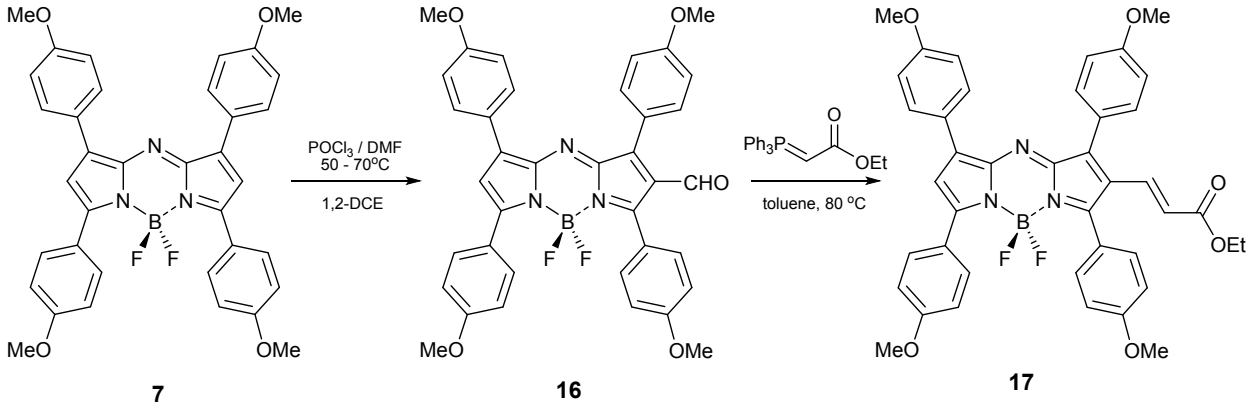

Scheme 6.

Wittig reaction with appropriate phosphonium ylides was employed to convert the resulting aldehyde **16** to a series of vinyl-ketones and esters **17** [48], or vinyl-esters conjugates[42] in 50-70% yields. This reaction uses mild reaction conditions (70ºC in toluene) and shows good compatibility with various functionalities. The Wittig products showed 3-30 nm low-energy shifts compared to 1,3,5,7-tetraaryl aza-BODIPY due to the enhancement of the π-system.

2.2.4. Derivatization at the boron hub. The first functionalization at the boron hub in aza-BODIPYs was reported in 2009 by O'Shea's group in an attempt to link tetraphenyl aza-BODIPY with alcohol-functionalized polystyrene beads.[49] The aza-BODIPY **18** was obtained by the room-temperature reaction in THF of parent aza-BODIPY **7** and sodium methoxide (generated in *situ* from methanol and sodium hydride, Scheme 7). Similar to BODIPYs, the introduction of the catechol fragment at the boron hub requires the use of aluminum chloride to activate B-F bonds before the formation of the catechol-bound aza-BODIPY **19**.[50] The fluorescence of the catechol-containing aza-BODIPYs, BODIPYs, benzo-fused aza-BODIPYs, and BOPHYs is completely quenched because of the efficient intramolecular charge-transfer from the electron-rich catechol fragment to the photo-excited chromophore.[50] Development of a family of constrained O-aza-BODIPYs based on intramolecular B-O chelation was reported by O'Shea's[51] and Hashimoto's[52] groups.

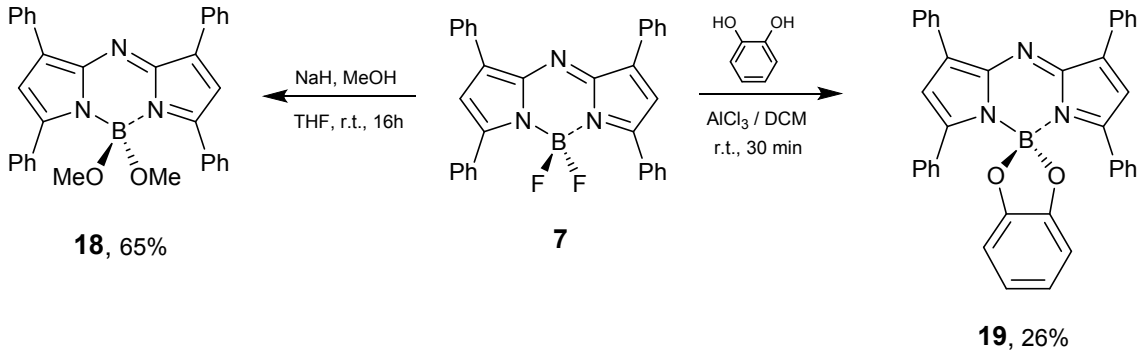

18, 65% **7** **19**, 26%

Scheme 7.

Nucleophilic attack of alkynyl- or aryl magnesium bromides is a standard synthetic strategy for the preparation of dialkynyl aza-BODIPY dyes (E-aza-BODIPY) or diaryl aza-BODIPY dyes (C-aza-BODIPY), respectively.[53,54] Aza-BODIPY **20** is stable under a weak acidic or basic conditions (Scheme 8). The E- and C-aza-BODIPYs **20**, **22**, and **24** feature 18-32 nm hypsochromic shifts in their absorption spectra and lower fluorescent quantum yields compared to the parent tetraphenyl aza-BODIPY.

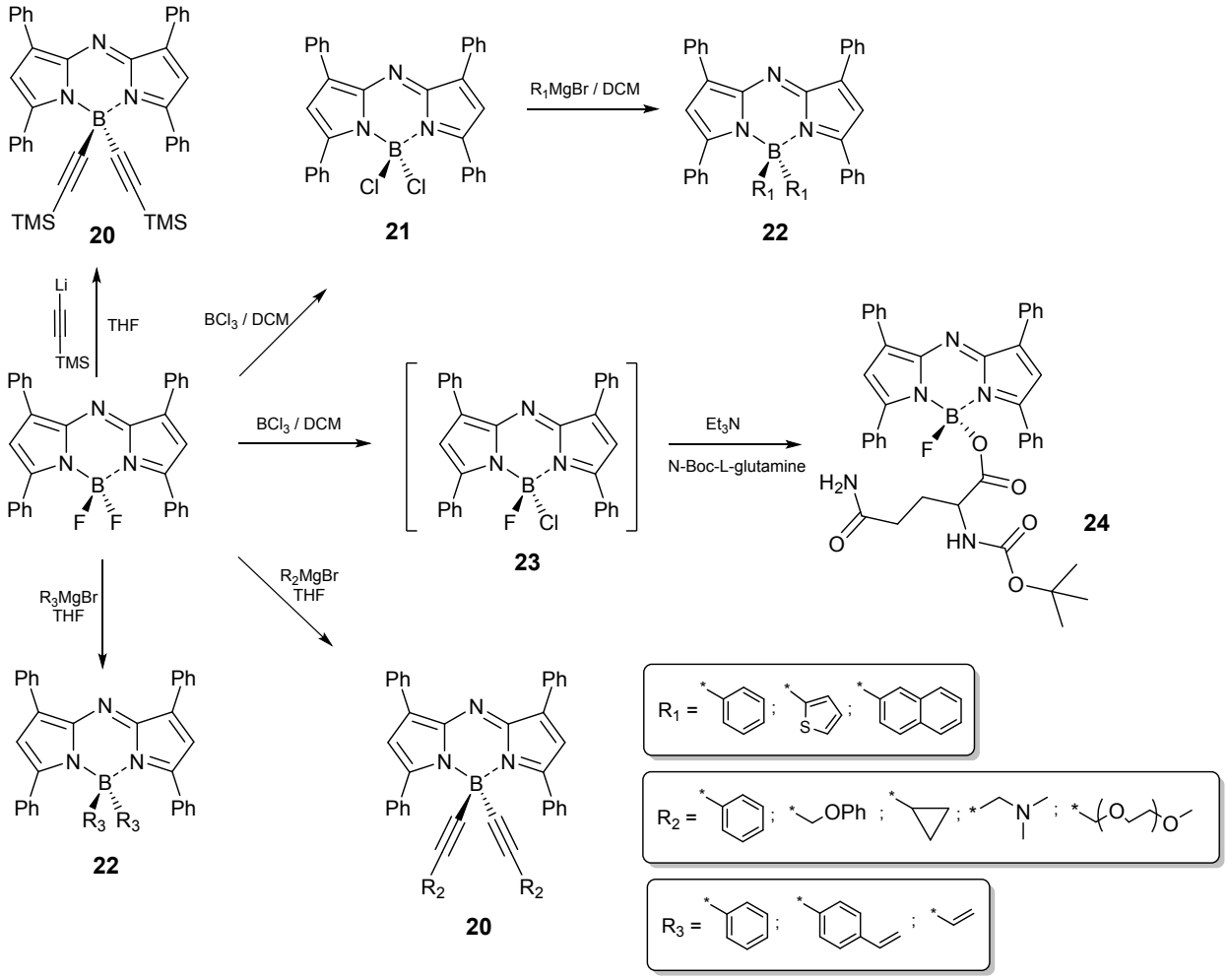

Scheme 8.

Since chloride anion is a better leaving group than the fluoride anion, the use of dichloroboron-aza-BODIPYs **21** and **23** can improve the synthesis of the aza-BODIPY derivatives functionalized at the boron hub (Scheme 8). In particular, this strategy allows to lower the molar ratio of Grignard reagent needed for the reaction as well as simplifies the reaction workup. Thus, phenyl, 2-naphthyl and 2-thienyl[55] C-aza-BODIPY derivatives were obtained using this methodology. This synthetic approach was also used recently for the preparation of the glutamic acid conjugates[56] **24** as well as arrays consisting of the aza-BODIPY chromophore and water-solubility enhancing unit attached to immunoglobuline molecule[57] or DOTA-monoamide chelated[58] Ga^{3+}.

2.3. Benzo-fused aza-BODIPYs.

Benzo-fused aza-dipyrromethenes were first prepared by Vollman in 1972 using the room-temperature reaction of arylmagnesium bromides and phthalonitrile in dry benzene. This synthetic strategy was exploited by Lukyanets in 2008[59] for the preparation of a series of benzo-fused aza-dipyrromethenes **28** and their BF_2 complexes **29**, **30** (Scheme 9). The expansion of π-system of the azadipyrromethene core leads to red-shifted absorption (712 nm) and emission (736 nm) as well as lowers the fluorescence quantum yield (Φ_F = 0.15) compared to the parent tetraphenyl aza-BODIPY **4**. Similar to the phthalocyanine derivatives, the introduction of the BINOL fragments to the isoindole groups (compound **30**) leads to the small low-energy shift of 25 (absorption) and 17 (fluorescence) nm.

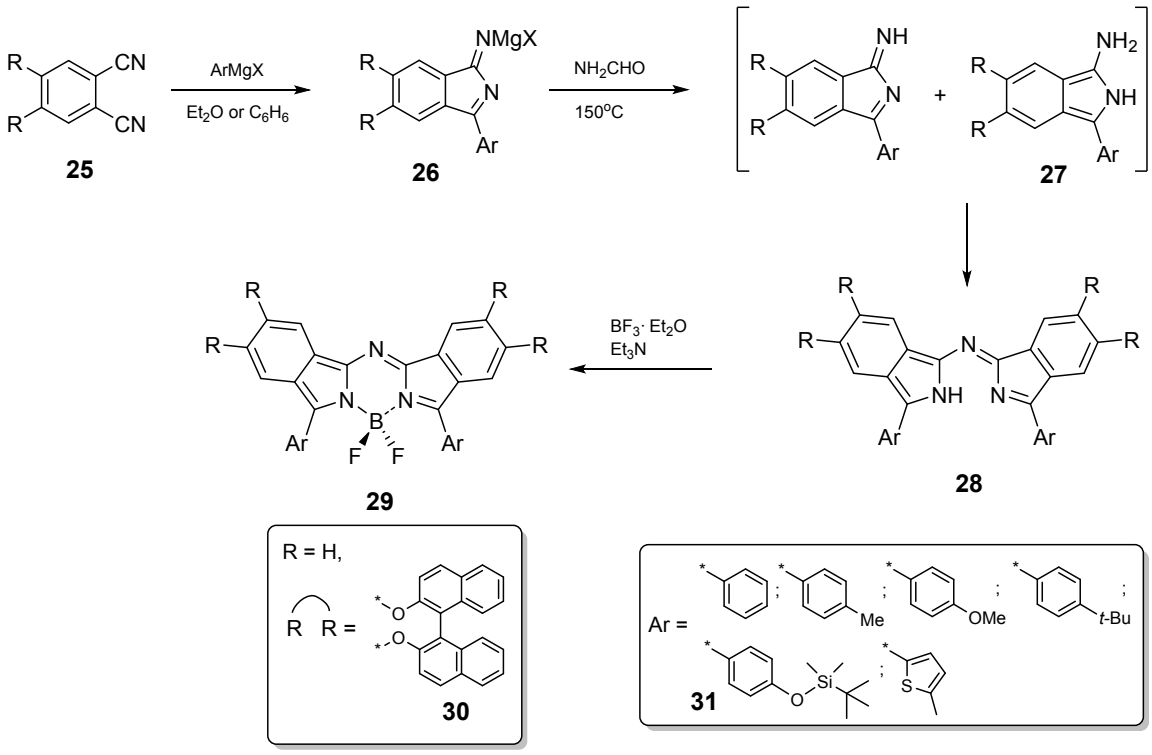

Scheme 9.

Use of an additional synthetic step (Leuckart-Wallach reduction by formamide to form **27**)[60] after the formation of intermediate **26** allowed increasing the yield of benzo-fused azadipyrromethenes to 56%. Preparation of benzo-fused aza-BODIPY through conventional nitroso derivative of 1-phenylisoindole was not successful because the reaction with nitrous acid leads to oxidative dimerization and isoindole ring opening. Using formamide employing route, a number of the benzo-fused aza-BODIPY dyes were synthesized including the first chiral aza-BODIPY derivatives **30** featuring one binaphthyl substituent.[61] Benzo-fused aza-BODIPY **31** with *tert*-butyldimethylsilyl groups at the phenyl substituents was used as a "turn-off" fluoride ion sensor in living HeLa cells.[62]

Zheng and co-workers have accidentally discovered a synthetic route to asymmetric benzo-fused aza-DIPY **32** via the reaction of phthalonitrile with potassium *tert*-butoxide in dry DMF (Scheme 10). The aza-DIPY **32** was prepared in 79% reaction yield.[63] An additional amino group at the α-position of the isoindole fragment could be further alkylated with alkyl halides and the BF_2 complex of the resulting compound could be obtained by the treatment with boron trifluoride etherate. The use of a stronger base, such as LDA, in the case of less reactive C-H bonds in benzonitrile **33**, leads to the formation of a series of 3,5-diaryl-benzo-fused azadipyrromethenes **35**.[64] In this reaction, first molecule of benzonitrile gets lithiated in ortho-position to the cyano group at low temperature to form **34**, before coupling with the molecule of second benzonitrile and formation of a benso-fused azadipyrromethene. Due to low solubility, BF_2 complexes could not be obtained except for the compound bearing a long alkyl chain on the phenyl fragment. However, zinc(II) complexes of **35** demonstrated strong absorption in the 621-653 nm region and no detectable fluorescence.

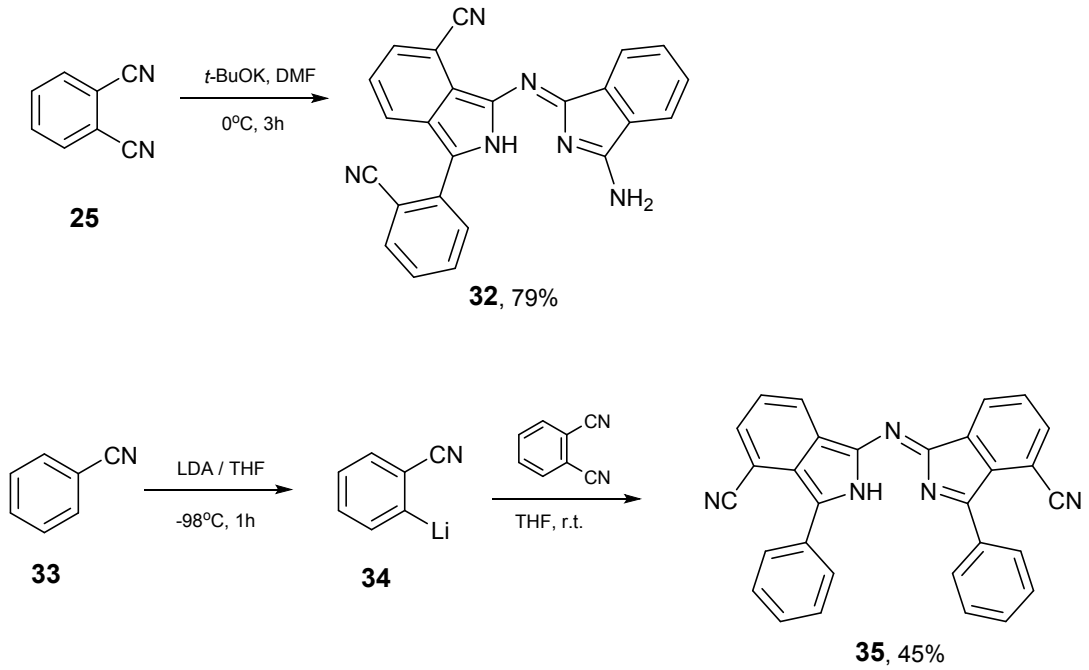

Scheme 10.

Benzo-fused aza-BODIPY with non-halogen substituents at the boron hub were synthesized using either the reaction of BCl_2 complex of aza-BODIPY **36** with Grignard reagent in 21% yield (**37**)[65] or the reaction of benzo-fused azadipyrromethene ligands **28** with 9-chloro-9-borafluorene in 89% reaction yield (**38**, Chart 2).[66] The introduction of borafluorene moiety did not affect the absorption and emission properties of the dye drastically, but improved its thermal stability. The ferrocene groups in **37** were found to be electronically coupled to each other despite a lack of through-bond conjugation and the Fe-Fe separation distance of ~10 Å. This

molecule is not fluorescent and forms an unusual aza-BODIPY-centered triplet state upon its photoexcitation.

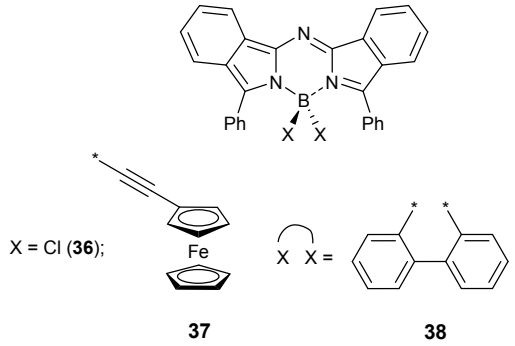

Chart 2.

The template synthesis of benzo-fused azadipyrromethene core was explored in 2016 by Ziegler and coworkers using Ph_3B and $BPh(OH)_2$ as templates and 1,3-diiminoisoindoline (DII, which can be considered as an activated phthalonitrile) as a building block.[67] The resulting "half-phthalocyanine" ("half-Pc") compound **39** with the terminal =NH or =O groups were found to accommodate planar geometry of the π-system core with boron substituents located perpendicular to the chromophore (Chart 3). A series of structurally similar compounds **40** were obtained using $Re(CO)_3$ as a template.

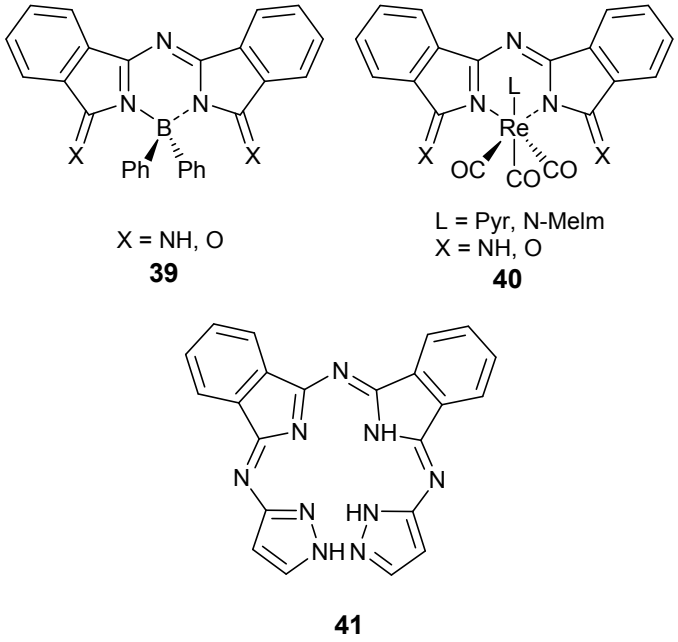

Chart 3.

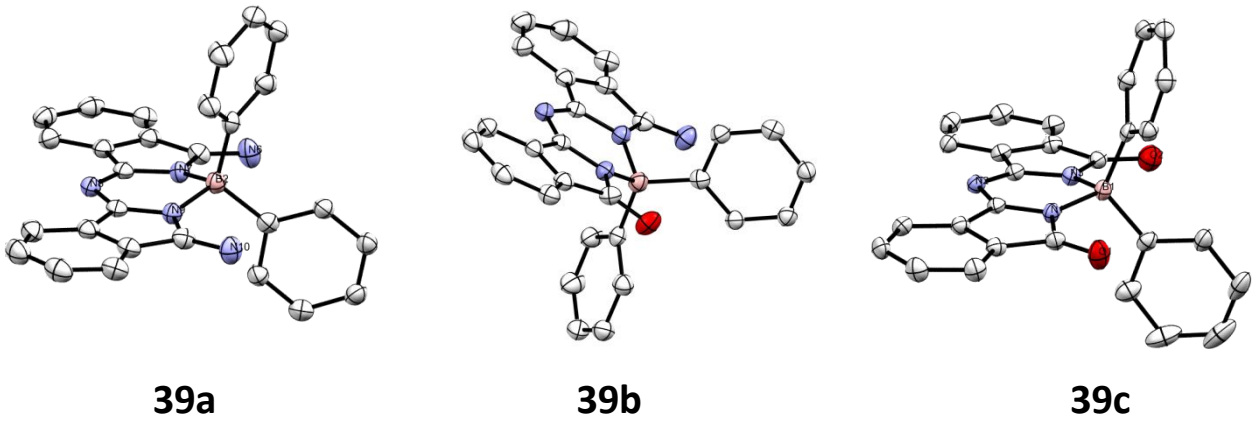

Figure 4. X-ray structures of the "half-phthalocyanines" **39**. Adapted from ref. 67 with permission from the Royal Society of Chemistry, copyright 2016.

The presence of five, highly-electronegative, nitrogen atoms in the core of **39** and **40** leads to the stabilization of HOMO orbital and, as a result, to a large high-energy shift (λ_{max} =333-348 nm) and lower extinction coefficient values for **39** and **40** compared to classic benzo-fused aza-BODIPY **29**.[68] It is interesting to note that the emission spectra of the compounds **39** were not the mirror images of the absorption spectra which usually is the case for most of BODIPY derivatives. Recently, the same group reported the synthesis of hemiporphyrazine-type chelate biliazine **41** (Chart 3) that is capable to form tetradentate transition metal complexes.[69] In this new platform, the chelate ring is closed via strong NH···N hydrogen bond (Figure 5). This hydrogen bond, however, is not strong enough to establish a completely conjugated macrocyclic chromophore system hence both free ligand and the complexes demonstrate UV-vis absorption profile similar to that of **39** and **40**. The electronic structure of the ligand in **39-41** can be considered as a two-electron oxidized derivative of classic benzo-fused aza-BODIPY core (18 *versus* 20 electrons). Further exploration of such modified azadipyrromethene core gave rise to two distinct families of compounds: core-modified aza-BODIPY analogues **44-45**[70] and the "Manitoba-dipyrromethenes" (MB-DIPY) compounds **47-48**[71] (Scheme 11). The synthesis of "Cammidge-type" aza-BODIPY analogues **45**, starts with the prepared in Cammidge laboratory precursor **42**. This precursor can be cross-coupled (under palladium-catalysed reaction conditions) with a variety of arylacetylenes to form aminoisoindoline **43**. Prepared from the aminoisoindoline **43** in a good yield, core-modified azadipyrromethenes **44** maintain *Z,Z*-configuration, while their BF_2 complexes **45** exist as an equilibrium mixture of *E*- and *Z*-isomers in solution. Again, the UV-vis spectra of **44** and **45** are close to those in "half-Pcs" **39** and **40**.

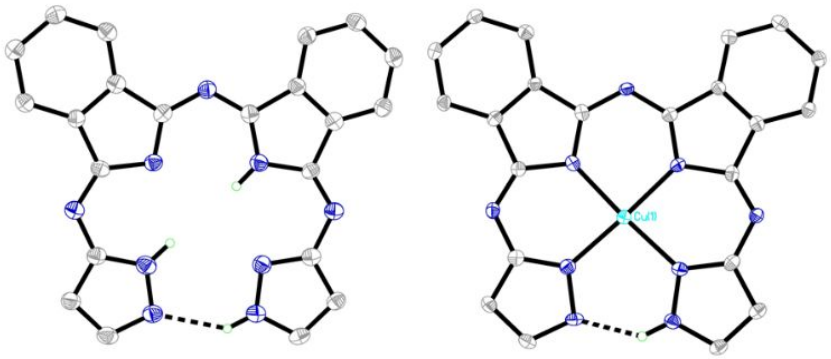

Figure 5. X-ray structures of the biliazine **41** and its copper complex. Reproduced from ref. 69 with permission from the Royal Society of Chemistry, copyright 2020.

The reaction between inexpensive phthalonitrile **25** and strongly basic carbon-centered nucleophiles, generated from the acetophenone precursors, results in the formation of iminoisoindoline derivatives **46** in excellent reaction yields.[71] The template self-condensation of **46** on sodium- or transition-metal ion leads to the formation of MB-DIPY derivatives **47** in which the central metal fits into N_2O_2 coordination sphere (Scheme 11). Carbonyl-containing MB-DIPYs feature *Z,Z*-configuration induced by hydrogen bonds for metal-free dyes and by tetradentate chelation for the metal complexes. In zinc, copper, nickel, cobalt, and iron MB-DIPY complexes that are already reported or currently being explored in our laboratory, the central metal ion fits into N_2O_2 coordination sphere of a single MB-DIPY ligand. However, when a larger silver(I) ion was used as a template, the formation of non-planar Ag_2(MB-DIPY)$_2$ system with a short Ag-Ag bond was observed.[72] Each of the MB-DIPY ligands in this structure adopts an orthogonal conformation, which points out to the geometrical flexibility of the MB-DIPY core. Extension of rigid π-system beyond the azadipyrromethene unit leads to the inception of a new chromophore with a visible-region maximum at 465-490 nm for **44** and at 450 nm for **48**. Zinc and sodium complexes **47** have their major absorption peaks around 580, 545 and 360 nm, and emission peaks around 600 nm. Two ferrocene groups in the ferrocenyl-substituted MB-DIPY **47d** are not electronically coupled with each other.[73] However, similar to the ferrocenyl-substituted aza-BODIPYs [27,28] and ferrocene-BODIPYs,[74] the UV-vis spectrum of this compound is enriched by the additional broad, low-energy, MLCT band.[73] In order to test the hypothesis that the compounds **39**, **45**, and **47** can be viewed as the two-electron oxidized forms of the regular benzo-fused aza-BODIPYs, the compounds **48** was reduced with sodium triacetoxyborohydride (STAB) in toluene to form of B,O-chelated aza-BODIPY derivatives, which were proven to be unstable for isolation but stable enough to be characterized by UV-vis and mass spectroscopy. As expected, two-electron reduced B,O-chelated complex of **48** had a strong absorption peak in the NIR region observed around 850 nm.

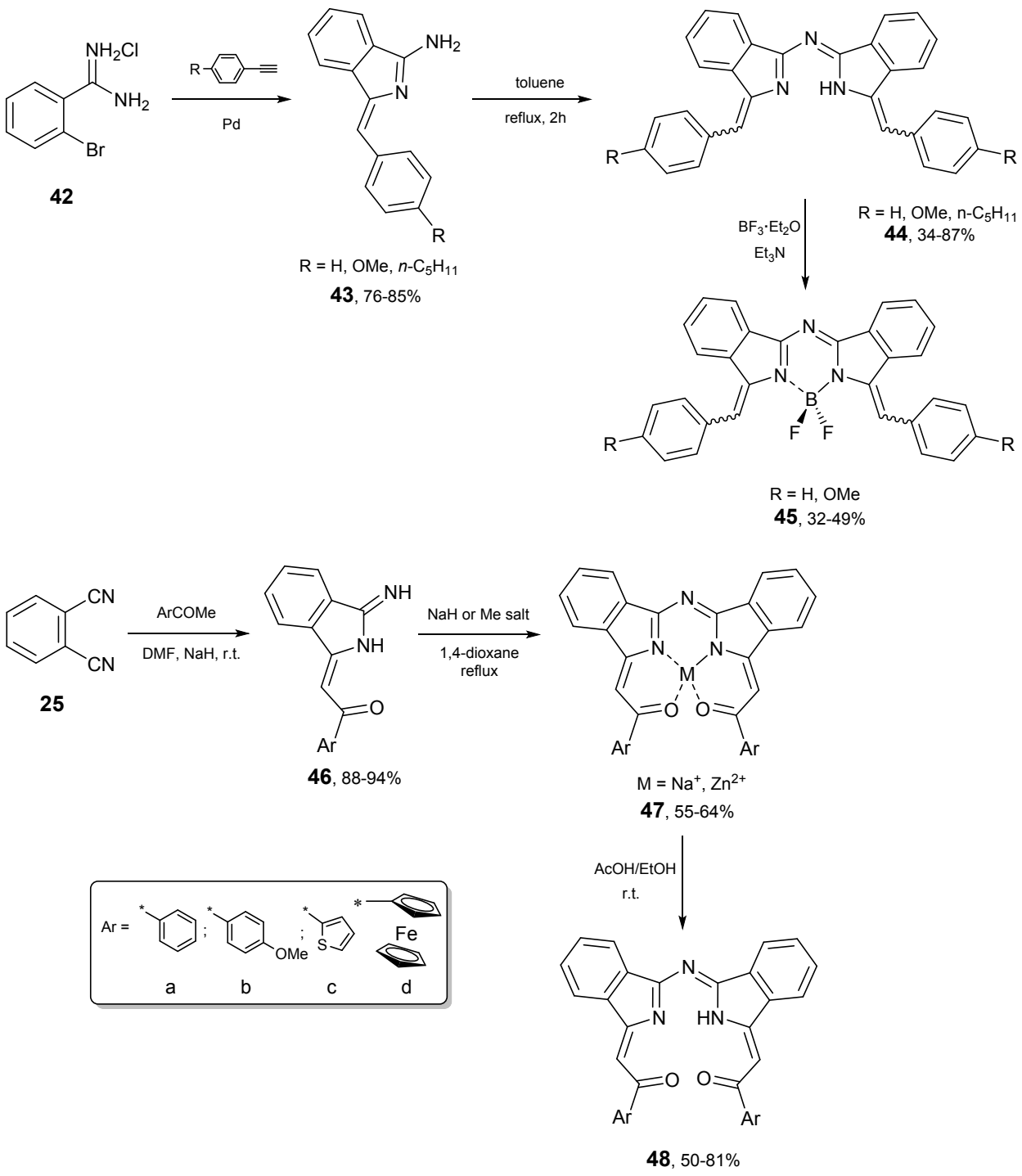
NH2Cl
NH2
Br
42
R
Pd
NH2
N
R
R = H, OMe, n-C5H11
43, 76-85%
toluene
reflux, 2h
N
N
HN
R
R
R = H, OMe, n-C5H11
44, 34-87%
BF3·Et2O
Et3N
N
N
N
B
F
F
R
R
R = H, OMe
45, 32-49%
CN
CN
25
ArCOMe
DMF, NaH, r.t.
NH
NH
O
Ar
46, 88-94%
NaH or Me salt
1,4-dioxane
reflux
N
N
N
M
O
O
Ar
Ar
M = Na+, Zn2+
47, 55-64%
AcOH/EtOH
r.t.
N
N
HN
O
O
Ar
Ar
48, 50-81%
Ar =
OMe
S
Fe
a
b
c
d

Scheme 11.

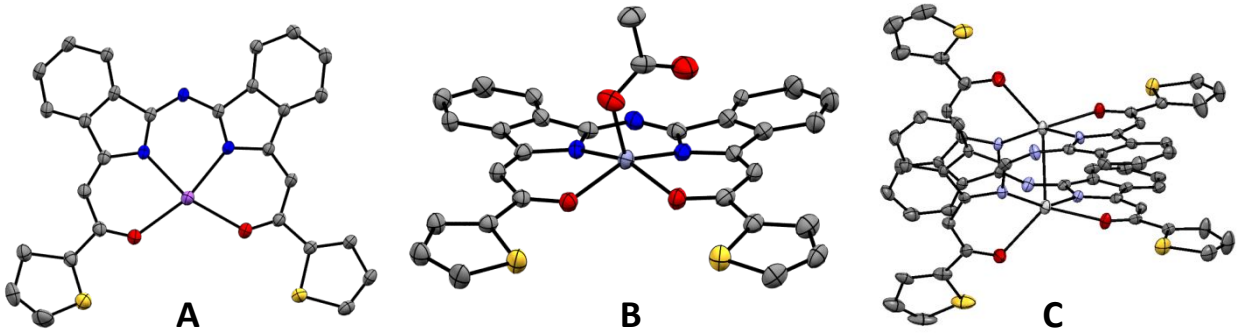

Figure 6. X-ray structures of sodium (**A**), zinc (**B**), and silver (**C**) MB-DIPYs **47**.[71,72] Adapted from ref. 71 and 72 with permission from the American Chemical Society and Royal Society of Chemistry, copyright 2019.

Three types of semihemiporphyrazine structures were obtained with pyridine, thiazole and benzimidazole fragments as the alternate heterocycles to the isoindoline unit in benzo-fused aza-DIPYs.[75] These systems are, however, rather poor chromophores with the rhenium(I) complexes **51** having a main absorption band at ~370 nm (Scheme 12).

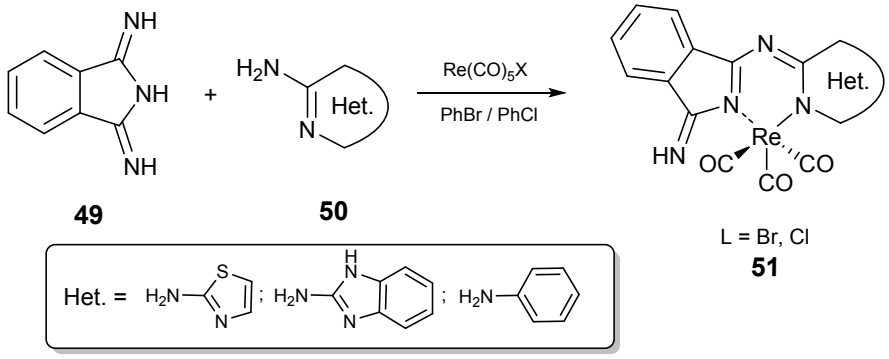

Scheme 12.

A novel type of dibenzothiophene [b]-fused core-expanded azaBODIPYs were obtained through an efficient post-functionalization of tetrabrominated azadipyrromethenes, using copper(I)-catalyzed cyclization, followed by BF_2 complexation.[76] These dyes show nearly planar skeletons, strong NIR absorption with maximum peaks up to 733 nm, and a remarkable low-lying LUMO level of -4.15 eV.

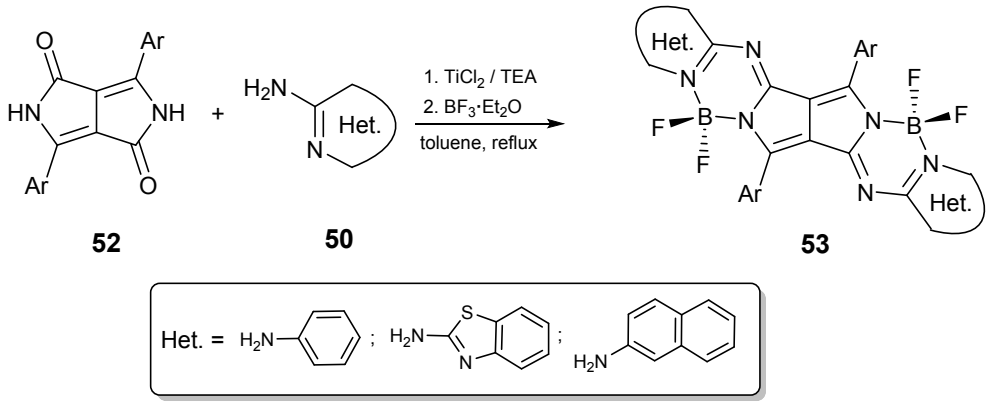

Scheme 13.

Kobayashi and coworkers have developed a synthetic strategy for the preparation of benzo- and heteroaromatic aza-BODIPYs through a Shiff base forming reaction of lactams and heteroaromatic amines.[77] A variety of lactams including benzo[c,d]indole, benzodipyrrolidone[78] and diketopyrrolopyrrole **52**[79] were converted to aza-BODIPY analogues. Dimeric aza-BODIPY structures formed in the latter two cases (**53**, for diketopyrrolopyrrole derivatives, Scheme 13) in a moderate yield (18-44% for octyloxy derivative of benzodipyrrolidone aza-BODIPY) exhibit intense absorption at around 650 nm and a mirror-imaged fluorescence in the far-red region with high fluorescence quantum yields of Φ_F = 0.81-0.87. Further modification of pyrrolopyrrole aza-BODIPY analogues was achieved through Suzuki-Miyaura and S_NAr reactions[80] in the construction of acceptor–donor–acceptor triads for organic photovoltaics application.[81]

2.4. BOPHY

2.4.1. Direct synthesis. Another type of unique pyrrole-BF_2-based fluorophore is bis(difluoroboron)1,2-bis((1H-pyrrol-2-yl)methylene)-hydrazine (BOPHY). This chromophore has two boron atoms per molecule and was independently reported by Ziegler[82] and Hao[83] in 2014. Condensation of pyrrole-2-carbaldehyde **54** with hydrazine hydrate using a catalytic amount of acetic acid gives dipyrrolohydrazine structures **55** in high reaction yields. These compounds readily react with boron trifluoride etherate to form the BOPHY chromophore **56** (Scheme 14). In the solid state, a BOPHY core is essentially planar although hydrazine Shiff base moieties retain double- and single bond character indicating the lack of delocalization in the tetracycle (Figure 7). The unsubstituted BOPHY exhibits absorption maxima at 424 and 442 nm, with extinction coefficients of 4.09×10^4 and 3.86×10^4 M^{-1} cm^{-1}, respectively, and two emission bands, at 465 and 493 nm[82]. First photophysical studies of unsubstituted and tetramethyl BOPHys were conducted in 2015 by Ziegler's group.[84] A notable feature of BOPHY compared to BODIPY is that all their derivatives synthesized thus far exhibit a broad absorption

spectrum and poor mirror symmetry between absorption and fluorescence spectra.[85] A comparative study of a set of related compounds in toluene demonstrated that BOPHY chromophores display a more intense fluorescence signal than related BODIPY chromophores across the green-red region of the visible electromagnetic spectrum, but the former shows less efficient lasing performance under the required strong irradiation regime[86]. The parent BOPHY and its alkyl or aryl derivatives have excellent fluorescence quantum yields that are close to unity.[82]

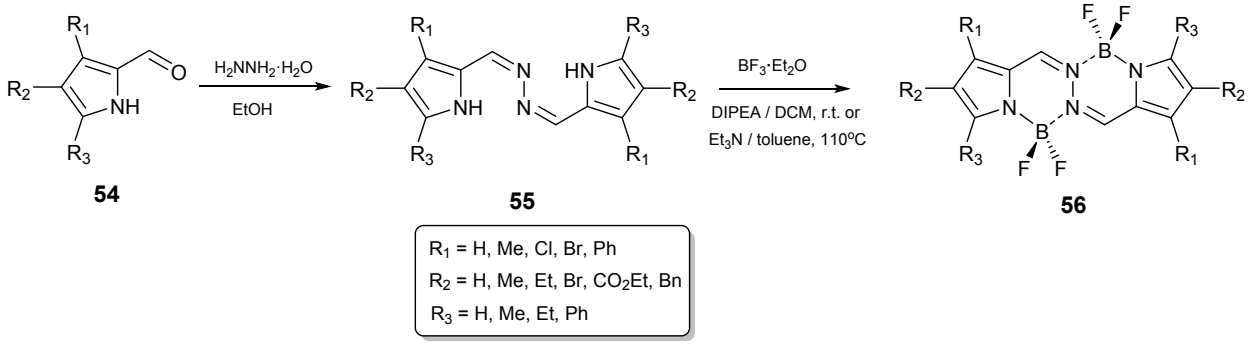

Scheme 14.

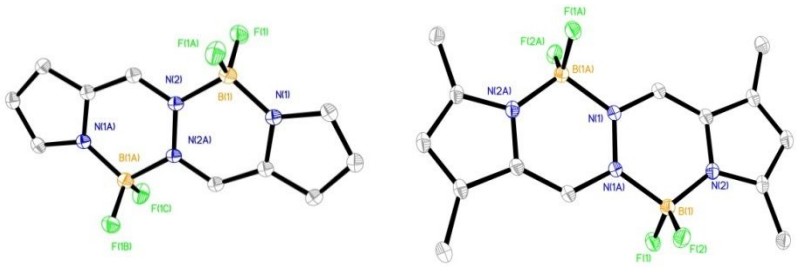

Figure 7. Representative examples of the X-ray structures of BOPHY. Adapted from ref. 82 with permission from the American Chemical Society, copyright 2014.

Dichloro-, [87]tetramethyl- and α-diester-, [83] dibromo- and tetrabromo-,[88] as well as tetraphenyl-[89] and dibenzyl-substituted BOPHYs[90] were synthesized from their respective substituted pyrroles in good yields. The introduction of substituents retains a high fluorescence quantum yields for the products even in the case of dichloro- and tetrabromo-BOPHY (85% and 61%, respectively), although only 20% quantum yield was reported for dibromo-BOPHY derivative.

2.4.2. Postfunctionalization.

2.4.2.1. Halogenation. Similar to BODIPY and aza-BODIPY chromophores, a BOPHY

molecule can be used in the reaction with electrophiles yielding halogenated and formylated derivatives. Regioselectivity of halogenation of parent (unsubstituted) BOPHY molecule **57** was explored by Hao's group (Scheme 15).[88] As expected for the pyrrole derivatives, the degree of halogenation of BOPHY depends on the amount of used halogenation agent and is ranges from β-monobrominated (obtained using 3 eq of Br_2) to hexabrominated (obtained using 300 eq Br_2). Unlike BOPHY, its synthetic precursor **55** is highly reactive towards bromine allowing the synthesis of its derivative with only 20 eq of bromine. In the case of tetramethyl-substituted BOPHY, both bromination and iodination products can be obtained in the presence of either NBS or NIS at room temperature.[91] 2,7-Diiodo-tetramethylBOPHY was also obtained using ICl as a reactant in polar solvents at the room temperature,[92] as well as with I_2 as the reactant with iodic acid in ethanol at 80ºC.[93] 2,7-Dibromotetraphenyl BOPHY derivative was synthesized by Zhao's group.[89]

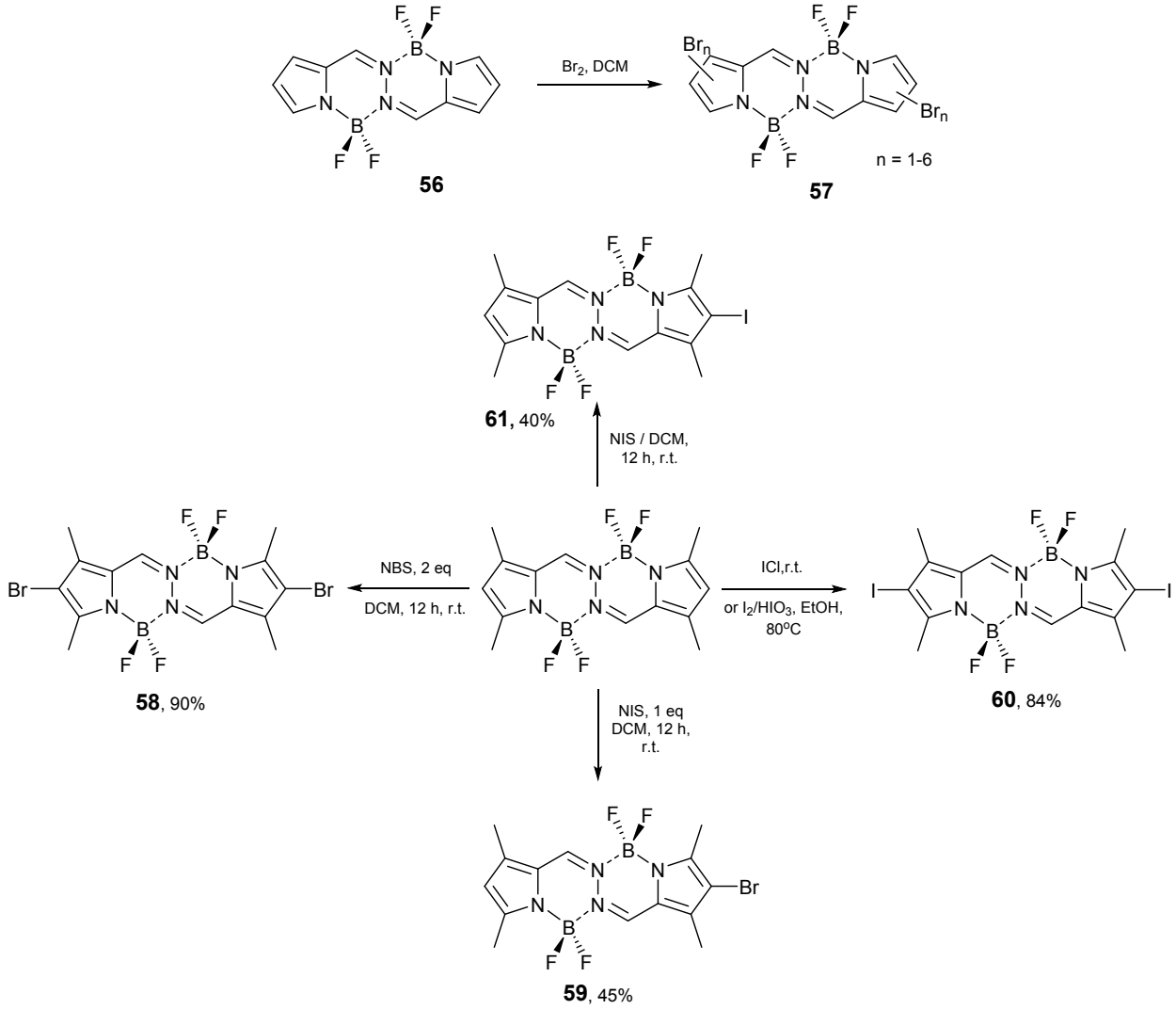

Scheme 15.

Halogenated derivatives of BOPHY display a low-energy shift of their absorption maxima for each halogen atom introduced due to their electron-withdrawing effect. The presence of halogen substituent also favors intersystem crossing to the triplet state, resulting in the drop of the fluorescence quantum yield (observed to a lesser extend for poly-halogenated BOPHYs). Good single oxygen generating ability of 2,7-dibromotetraphenyl BOPHY[89] as well as 2,7-diiodotetramethyl BOPHY **60**[94] was also documented. Moreover, compound **60** was employed in a triplet-triplet annihilation photon upconversion cascade using 9,10-diphenylanthracene as emitter.[94] This system was successfully used for metal-free, visible light, room-temperature C-C coupling catalysis.[93]

2.4.2.2. Nucleophilic substitution. Halogenated derivatives of BOPHY are valuable precursors for further functionalization. The nucleophilic substitution of chlorine atoms in 3,8-dichlorotetraphenylBOPHY with *O*-, *N*- and *S*-nucleophiles was performed in boiling acetonitrile using triethylamine or potassium carbonate as a base with up to 88% yield of 3,8-dipiperidyl-3,8-dialkylsulfanyl-, and 3,8-diphenoxy-substituted BOPHY derivatives.[87] *n*-Butylamine, pyrrole, 4-*tert*-butylaniline, and diethylamine can be used as the nucleophiles for the preparation of a series of 3- or 3,8-disubstituted BOPHYs in 1,2-dichloroethane or toluene under elevated temperatures. Interestingly, in the case of the polybrominated BOPHYs, a nucleophilic substitution of bromine occurred first at 3,8-positions, whereas 2,7-positions were unreactive under these conditions.[88] In general, the introduction of amine or pyrrole moieties weakens the fluorescence of the product which is, quite likely, reflective of photo-induced electron-transfer process from these groups to the photo-excited BOPHY core. Upon the introduction of substituents, the molecular structure of BOPHY core undergoes a transformation from the almost planar to highly twisted conformation with dihedral angle between two pyrrolic units of 33.2º observed for 3,8-diaminoBOPHY[88] and 39º observed for 3,8-distyryl BOPHY.[92]

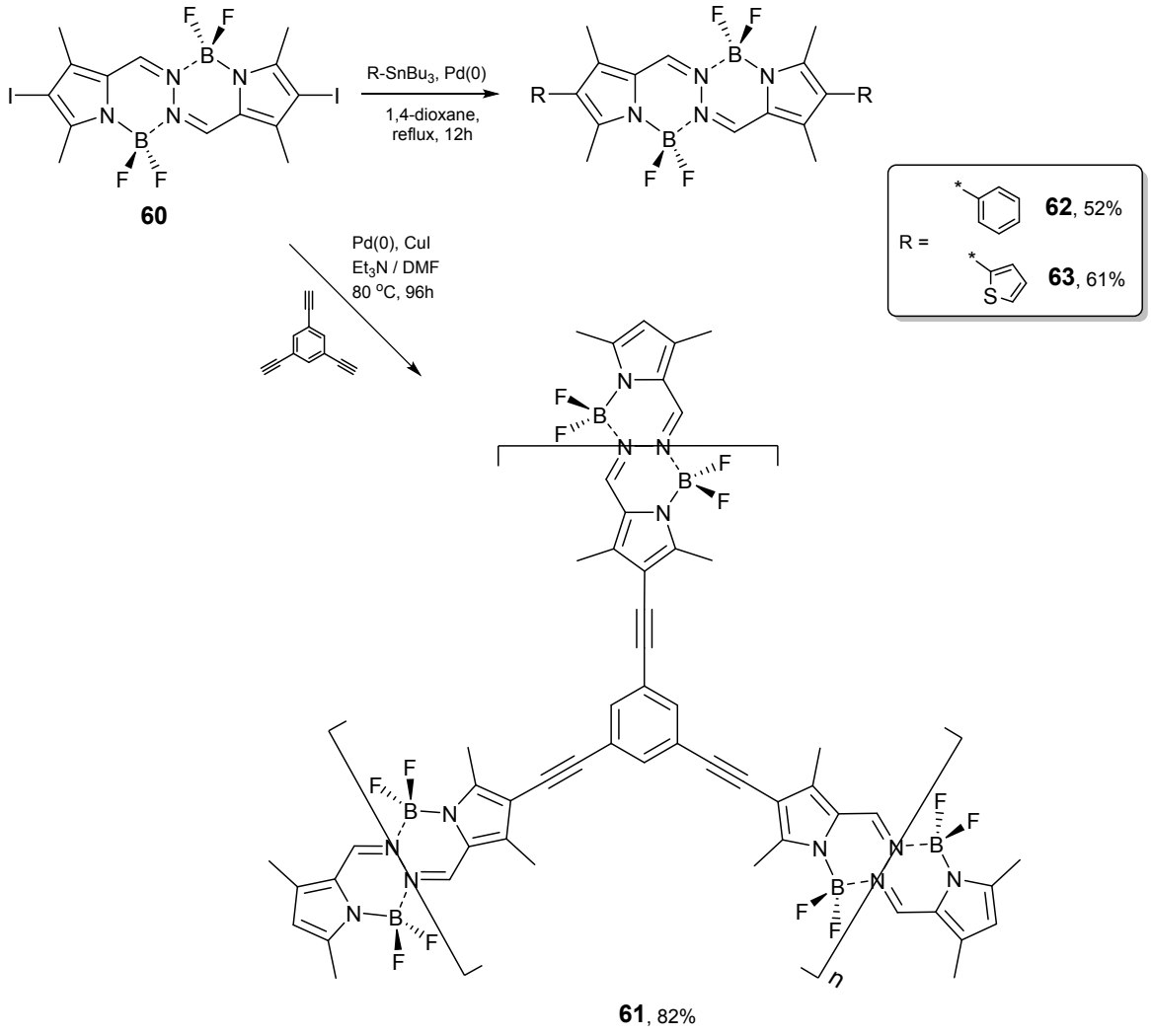

Scheme 16.

2.4.2.3. Coupling reactions. Extension of a π-system and a bathochromic shift of absorption and emission maxima of BOPHY chromophore can be achieved using palladium(0)-catalyzed cross-coupling reactions. For instance, 3,8-dichloroBOPHY was coupled with 1-butyl-4-ethynylbenzene in Sonogashira reaction conditions to give disubstituted product in 39% reaction yield.[87] 3,8-Dibromo-substituted BOPHY underwent coupling with 4-dimethylaminobenzene boronic acid in a Suzuki reaction conditions to form the disubstituted product in 83% yield.[88] Both 3,8-dichloro- and 3,8-dibromo- precursors react with 2-(tributylstannyl)thiophene in a Stille coupling reaction. Compounds **58** and **60** were introduced in Sonogashira reaction by Son's group.[91] The same reaction was employed for the construction of the porous conjugated polymers based on **60** and 1,3,5-triethynylbenzene (polymer **61**) or 1,3,5-tris(4-ethynylphenyl)benzene (Scheme 16).[95] BOPHY-based polymers were used as heterogeneous photocatalysts in the oxidation of sulfides to the corresponding sulfoxides.

Conjugated porous polymers(CPPs) based on BOPHY moiety have shown higher hydrogen evolution rate than TiO_2, the most studied inorganic semiconductor as photocatalyst in the hydrogen production reaction.[96] Phenyl- (**62**) and thienyl- (**63**) substituted BOPHYs generated in Stille reactions from **60** demonstrated different kinds of aggregation in solid state and solution: BOPHY **62** demonstrates H-aggregation, and the thienyl-substituted BOPHY **63** induces emission enhancement (AIEE) due to the formation of J-aggregates which results in narrow, red-shifted and enhanced emission.[97]

2.4.2.4. Knoevenagel condensations. Unlike aza-BODIPYs, which 3,5-dimethyl derivatives are still unknown, BOPHYs can have methyl groups at the α-pyrrolic positions, which renders them reactive for the Knoevenagel condensation reaction. The typical protocol consists of using high temperature, piperidine as a base, toluene as a solvent, and trace amounts of *p*-TsOH as an activator (Scheme 17). Depending on the arylaldehyde nature and amount, either 3-mono or 3,8- bis-substituted BOPHY is obtained as a major product during the reaction and is purified by chromatography. The introduction of styrylic substituents generally leads to the low-energy shift of the absorption and emission maxima. Compared to the absorption of tetramethyl-containing BOPHY (λ= 444 and 467 nm in DCM[82]), the lowest-energy π-π* transition shifted by 128 and 159 nm, respectively, for BOPHY dyes **64** functionalized at the 3,8-positions with vinylthiophenes,[98] and by 113 and 159 nm, respectively, for dyes **65** and **66** (in THF).[92] Introduction of the vinylferrocene fragment in **67** red-shifts the longest wavelength maximum (predominantly MLCT in nature) by 227 nm (in DCM) while simultaneously quenching the fluorescence and establishing long-range metal-metal coupling with 200 mV separation between the ferrocene-centered oxidation waves.[99] Knovenagel condensation products of BOPHY generally exhibit a larger red-shift in absorption maxima (up to 230 nm) compared to C-C coupling products (up to 150 nm).

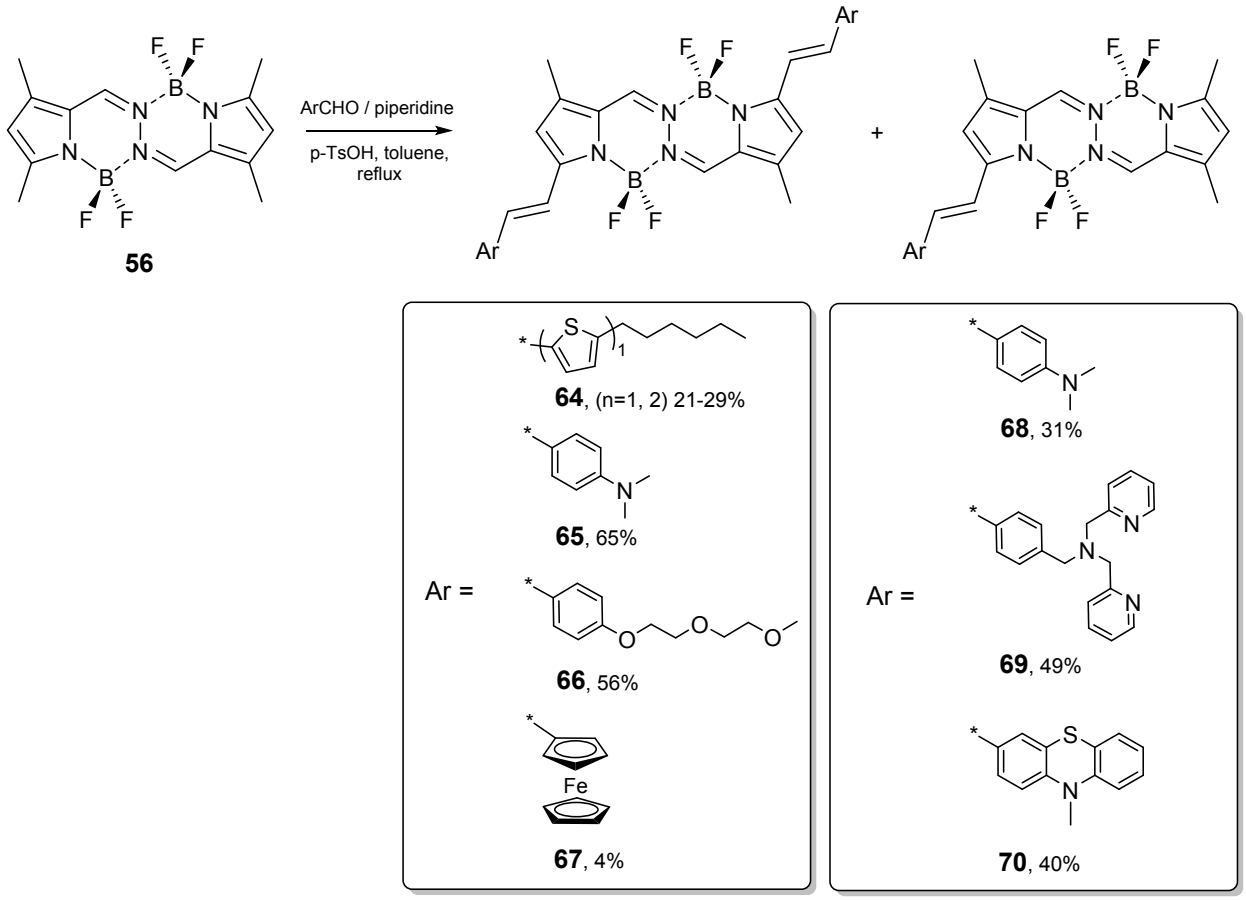

Scheme 17.

The ability of the mono-substituted BOPHYs **68-70** to change their fluorescence upon protonation or complexation with cations was studied by groups of Xiao (protonation of BOPHY **68**),[100] Zang (complexation of Cd^{2+} to BOPHY **69**)[101] and Yu (complexation of Cu^{2+} to BOPHY **70**).[102] Zhang and Zhao reported of a series of mono-substituted with several aryl fragments photosensitizers prepared by the Knoevenagel condensation from 2,7-diiodotetramethyl BOPHY.[94] Photobleaching of the compound **66** in thin plastic films,[103] as well as lack of interaction of the flanking *N,N*-dimethylanilino groups in compound **68**,[104] and effect of temperature and solvents on the various spectroscopic properties of unsubstituted and tetramethyl BOPHYs[105] were studied by Ziessel and coworkers. An attempt of the introduction of cyano group at the *meso*-carbon atoms of BOPHY core resulted in a partial extrusion of the BOPHY core (Figure 8) and drastic reduction in the fluorescence quantum yield.[106]

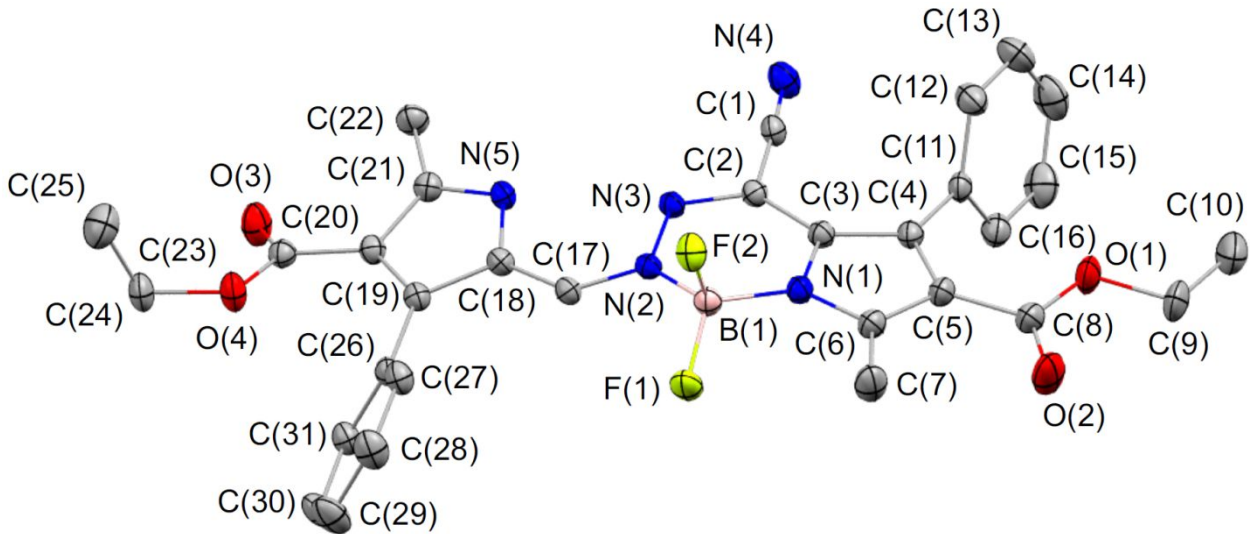

Figure 8. X-ray structure of mono-borylated BOPHY.[106] Adapted from ref. 106 with permission from Wiley, copyright 2017.

2.4.2.5. Formylation. Tetramethyl-substituted BOPHY was successfully formylated at the α-position (BOPHY **71**) in 72% reaction yield (Chart 4). The Vilsmeier-Haack reaction conditions with Vilsmeier reagent generated *in situ* were used in this approch.[107] Further derivatization with azine fragment renders it a sensitive and selective sensor for Cu^{2+} ion.

2.4.2.6. Derivatization via fluorine displacement. The reaction of pyrrolo-imine **55** with triphenylborane in refluxing toluene gives complex **72** in 34% yield (Chart 4). Interestingly, the five-membered ring of bis-(diphenylboron) complex **73** is formed in the case of tetramethyl-substituted BOPHY in 61% yield because of the steric hindrance created by the methyl group in the core structure and phenyl groups in the BPh_2 fragments. Both complexes are strongly emissive with quantum yields in the range of 0.52–0.88 with a maximum peak at 513 nm for **72** and 547 nm for **73** in DCM.[108] Chiral BINOL-based O-BOPHYs have been prepared in 35% yield from the respective BF_2 precursors.[109] Similar to the aza-BODIPY chemistry, the authors used the activation of the B-F bonds by aluminum chloride as a Lewis acid.

2.4.2.7. Ring-fused BOPHYs. Ring-fused BOPHYs were synthesized from respective indole[83], thieno- and furopyrroles in an attempt to prepare long-wavelength fluorescent dyes by extending the conjugation of the π-system. The β-thiophene-fused BOPHY **74** (Chart 4) in DCM showed strong emission in the NIR region (λ_{abs} = 610 nm, λ_{em} = 648 nm, Φ_F = 0.50). Its emission peak shifts to 717 nm in solid state.[110] Cyclic voltammetry and DFT calculations showed that the

aromatic ring fusions destabilized the HOMO energy, confirming the effective expansion of π-conjugation over these BOPHY dyes. Solvatochromic effects were studied by Zhou and co-authors for the furan-fused BOPHYs.[111] As expected for the chromophore-based π–π* transitions, the solvatochromic effect in **75** is rather small. Indeed, the absorption maximum of **75** is 608 nm in toluene and 594 nm in DMSO (388 cm^{-1}).

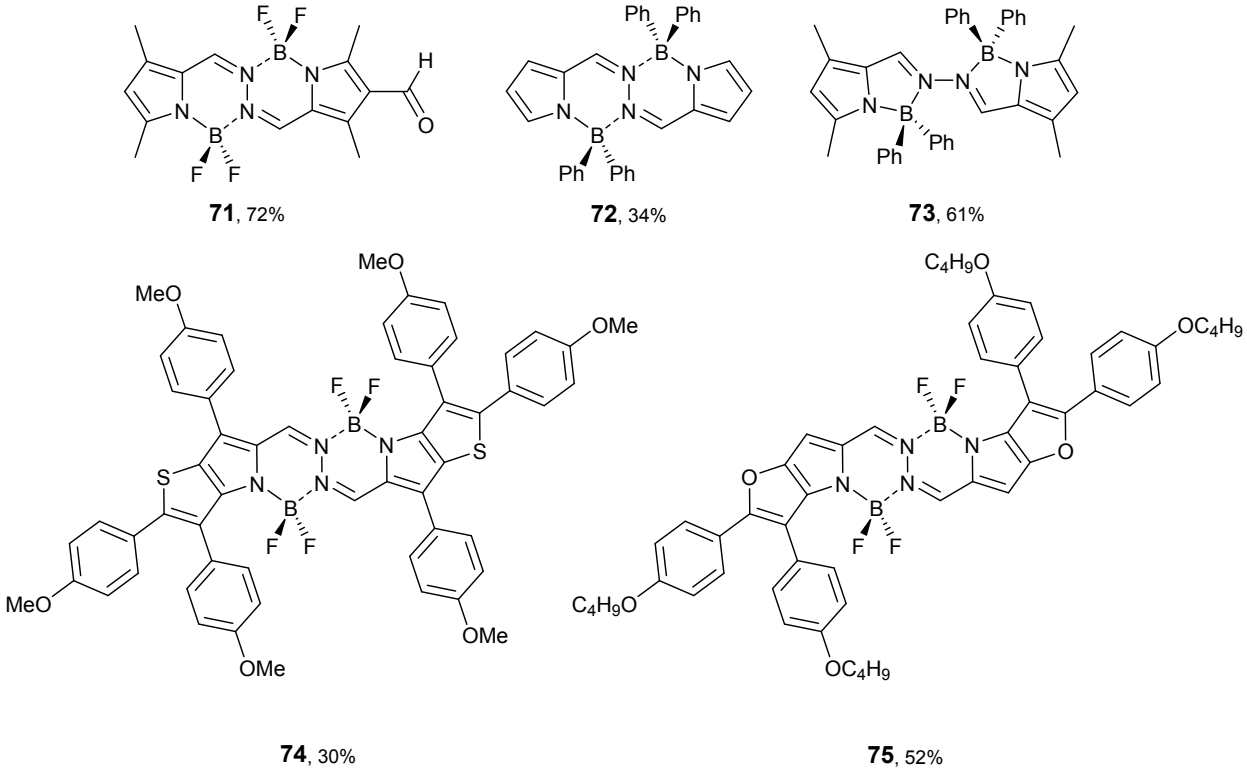

71, 72% **72**, 34% **73**, 61%

74, 30% **75**, 52%

Chart 4.

2.5. Other BOPHY analogues

Although highly spectroscopically efficient and stable, the aza-BODIPY and BOPHY platforms' main disadvantage is that they originate from highly symmetric and rigid cores. Such an origin narrows Stokes shifts and makes them prone to quenching particularly in high concentration and in a solid state. Thus, it is not surprising to see the raise of a series of asymmetric fluorophores that have been proposed to overcome such shortcoming by lowering the pseudo-C_2-symmetry of the molecule thereby inducing large redistribution in charge upon excitation (Scheme 18).

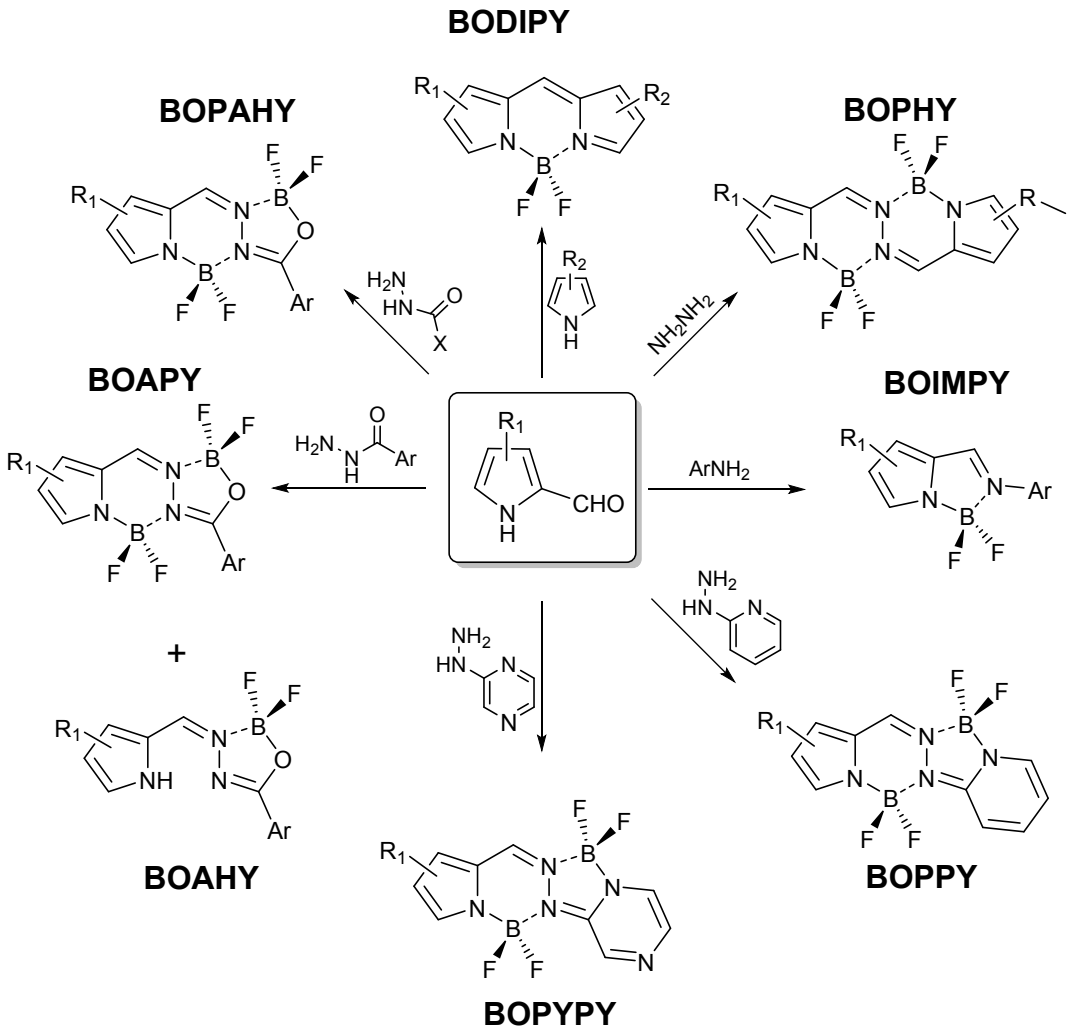

Scheme 18.

2.5.1. BOIMPY. A series of air-stable BOIMPY (BOron complexes of IMinoPYrrolide ligands) fluorophores were prepared in two steps. The first step is a simple condensation of the pyrrole-2-carboxaldehydes **76** with aromatic amines, which results in the formation of the ligand **77** in 64-87% reaction yield (Scheme 19). The reaction of the ligands with boron trifluoride etherate leads to the formation of BOIMPYs in 52-83% yields.[112] Complexes **78**-**82** show the absorption maxima at 390-460 nm and emission maxima at 536-650 nm in acetonitrile thereby demonstrating Stokes shifts of up to 150 nm. The fluorescence quantum yields of BOIMPY dyes depended on solvent polarity, steric constraints of the substituents as well as protonation states. Interestingly, the non-emissive in solution BOIMPY **81** has enhanced fluorescence (Φ_F = 0.19) in the solid state due to restricted molecular motions and orthogonal arrangement of the ring systems that avoid close π-π contacts.

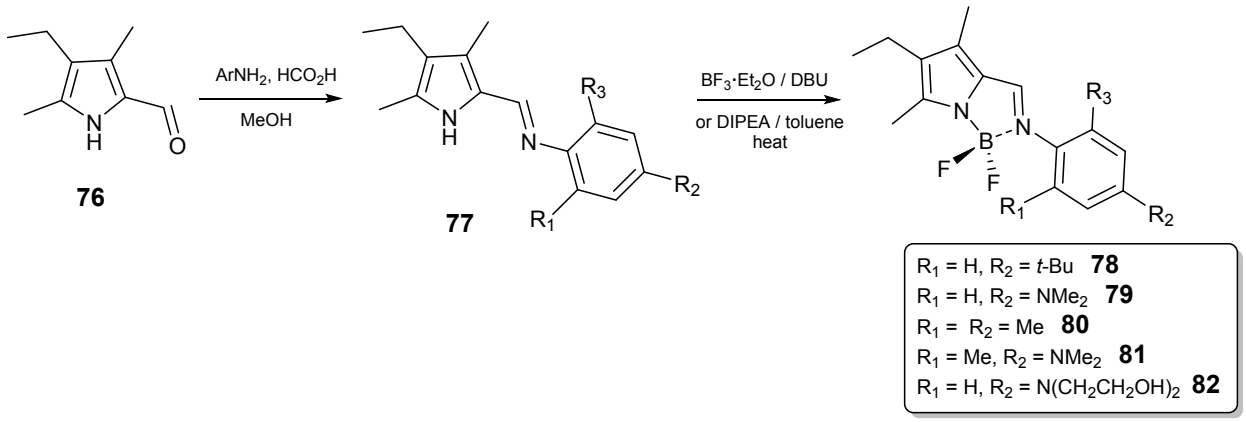

Scheme 19.

Halogen-substituted 2-(*N*-arylimino)pyrrolyl-BPh_2 complexes of BOIMPY **83-86** were recently used for the preparation of multi-layered organic light-emitting diodes (OLED, Chart 5).[113] The internal heavy-atom effect was controlled by the position of the halogen atom in the N-aryl ring of the ligand moiety, being negligible for the *para*-iodine substitution and most effective for the *ortho*-iodine substitution. Accordingly, complex **86** exhibited the greatest phosphorescence emission at 77 K. The OLEDs prepared with molecules **83**–**86** did not clearly show the phosphorescence contribution to the electroluminescence spectrum possibly because of a significant charge-induced triplet quenching, promoted by the long lifetime of the triplets.

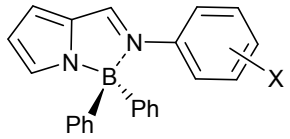

X = 4-I **83**
X = 3-Br **84**
X = 2-Br **85**
X = 2-I **86**

Chart 5.

2.5.2. BOIMPY. Another type of BODIPY analogues also named BOIMPY (bis(BOrondifluoride)-8-IMidazodiPYrromethene) **89** was designed in 2016 by Werz's group as a unique red-emitting highly fluorescent scaffold (Scheme 20).[114] The synthesis of the BOIMPYs relies on familiarity from the BODIPY's chemistry sequence. The first step involves the oxidation of the 2-hydroxymethylbenzimidazoles **87** to the respective carbaldehydes with orthoiodoxybenzoic acid (IBX). The resulting aldehydes were condensed *in situ* with 2-ethylpyrrole to give dipyrromethanes **88** in up to 59% yield. The dipyrrins formed after oxidation

with DDQ were found to be unstable and could not be isolated. Instead, two-fold BF_2 coordination was achieved at low temperatures (-78 ºC) using strong, hindered bases such as Schwesinger's noncationic phosphazene base (BEMP) to form the BOIMPY derivatives **89**. In these chromophores, absorptions and fluorescences are observed in the red region of the visible spectrum. In the case of unsubstituted BOIMPY **89**, the low-energy absorption peak was observed at 598 nm and the fluorescence peak was observed at 612 nm (Φ_F = 0.96 in DCM). A number of post-functionalizations were applied for these chromophores such as the tunable halogenations, the selective fluoride substitutions, and the variable one- or two-fold Knoevenagel-type condensations. Optical spectra and electronic structure of the obtained BOIMPYs have been modeled on TD-DFT[115] and CC2[116] level of theory.

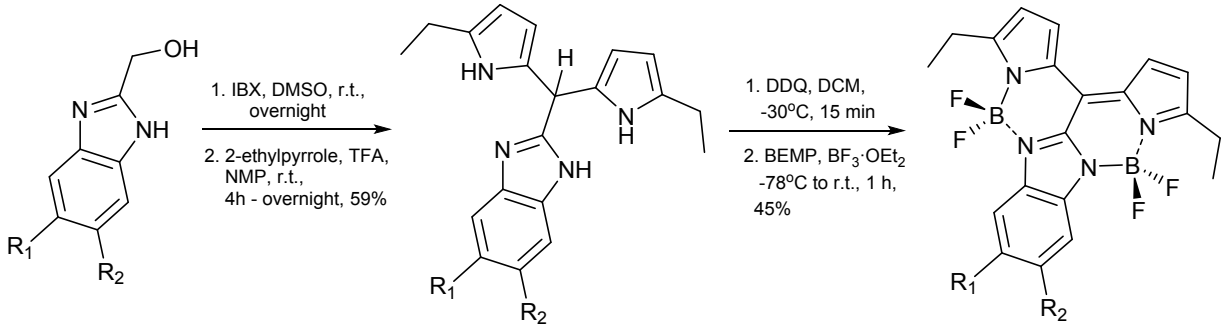

87 **88** **89**

Scheme 20.

Later on, the same group replaced benzimidazole fragment in BOIMPY with the tetrazole one. The tetrazole-containing analogue of BOIMPY (aza-BOIMPY) is also featuring twofold BF_2-complexation of dipyrromethene motifs.[117] A *meso*-tetrazole unit moves the scaffold towards unprecedented electron deficiency reflected in its low-lying LUMO compared to a BOIMPY platform. Two main quasi-reversible reduction potentials at -620 mV and -1370 mV (vs. Fc^+/Fc) were detected in cyclic voltammetry experiments. No oxidation processes were observed in the electrochemical experiments with both BOIMPY and aza-BOIMPY systems, which is reflective of the heavily stabilized HOMO. Aza-BOIMPYs are highly emissive (Φ_F of up to 0.82), absorption and emission events focus at roughly 600 nm with exceptionally small Stokes shifts (209 cm^{-1}) and high attenuation coefficients (up to 120,000 M^{-1} cm^{-1}) in DCM. Aza-BOIMPY system was further modified by the introduction of α-alkoxy- and β-aryl- (phenyl, thienyl and furyl) groups to create push-pull fluorophores.[118] This red-shifts the main absorption transitions to the deep NIR region from ca. 700 to 830 nm and gives rise to very high stationary dipole moments of up to 12.1 D, with inverted polarity compared to the related BODIPY frameworks.

2.5.3. BOPPY and BOPYPY. In 2018 Jiao's group reported a synthetic strategy for the preparation of an asymmetric bis(BF_2) fluorophores that contain both pyrrole and *N*-heteroarene fragments (BOPPY, Chart 6).[119] One-pot condensation of corresponding formyl-pyrroles with 2-hydrazinylpyridine in the presence of ptoluenesulfonic acid (PTSA) followed by the reaction with boron trifluoride etherate solution in the presence of *N,N*-diisopropylethylamine smoothly gives BOPPY fluorophores in 28-54% yield.

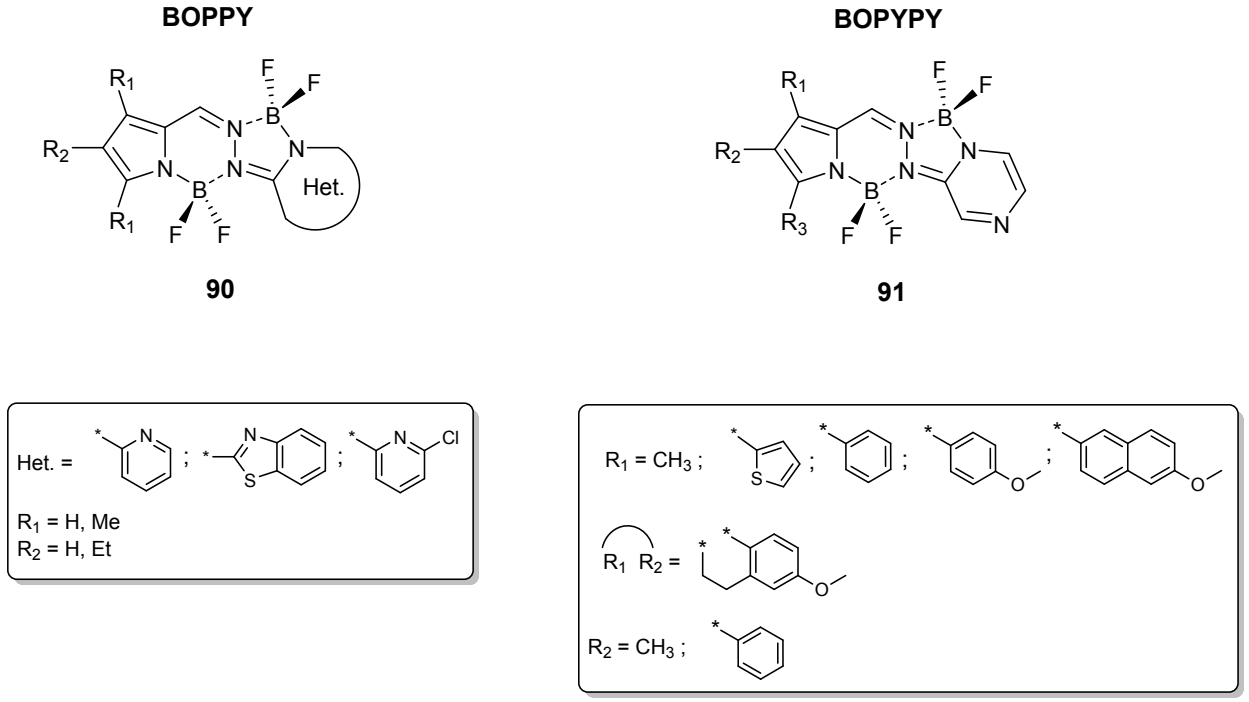

Chart 6.

BOPPYs **90** exhibit two well-split absorption maxima in the range of 380-430 nm and dual fluorescence emission maxima between 430-490 nm, with a fluorescence quantum yield ranging from 0.38 to 0.79 in dichloromethane. In the solid state, all of them adopt coplanar inclined arrangements of their transition dipoles with slip angles of 25.0°−35.8° characteristic of J-type solid-state packing which manifests in emission bands with maxima ranging from 466 to 625 nm that are significantly red-shifted with respect to their corresponding emission bands in solution. The α-pyrrolic chlorine atom in the BOPPY core was used for the facile postfunctionalization of these dyes. The nucleophilic substitution reactions with *n*-butylamine in the presence of a base in refluxing 1,2-dichloroethane generated *n*-butylamine derivative in 82% yield, while the thiophene substituted BOPPY was prepared by Stille cross-coupling reaction – in 91% reaction yield.

The introduction of an additional nitrogen atom in the heterocyclic moiety of tetracyclic

pyrazine/pyrrole-fused asymmetric bis(BF_2) fluorescent dyes (BOPYPYs) **91** was achieved by Zhao's group (Chart 6). The reaction pathway is similar to that used for the preparation of BOPPY except 1-(pyrazin-2-yl)hydrazine instead of 2-hydrazinylpyridine was used in the condensation reaction with pyrrole-2-carboxaldehyde.[120] The reported yields of this one-pot reaction were 35-41%. BOPYPYs with the extended π-system were prepared by the pyrrole fragment modification with the aryl moieties. Such an expanded systems exhibit red-shifted low-energy absorption (498–546 nm) and the emissions (560–610 nm) bands in DCM. Knoevenagel condensation of the BOPYPY's methyl group with 4-dimethylaminobenzaldehyde produced a pH-responsive fluorescent dye in 56% yield.

2.5.4. BOAPY, BOAHY and BOPAHY. In 2019, Jiao and coworkers designed a new family of the chromophores, difuoroBOronate anchored AcylHYdrazones (BOAHY, Scheme 21).[121] The synthesis of BOAHY **92** is a simple one-pot two-step reaction that utilizes a variety of the commercially available hydrazides and diverse aldehydes with $BF_3{\cdot}OEt_2$ in the presence of triethylamine. The overall yield of the reaction depends on the nature of hydrazine and aldehyde and varies between 48 and 82%. The optical properties on the BOAHY systems are quite tunable with the observed strong absorption band between 300 and 600 nm. However, BOAHYs are poor fluorophores in solution. Their solid powders and films, on the other hand, show strong fluorescence emission and are brilliant under 365 nm hand-held UV lamp irradiation, with fluorescence quantum yields of up to 0.62. Although these systems are rigidified with BF_2 fragment, these compounds may still rotate around their C=N bonds upon photoexcitation. This photoisomerization causes obvious absorption or fluorescence changes in BOAHY **92** solution and is reversible in a dark environment.

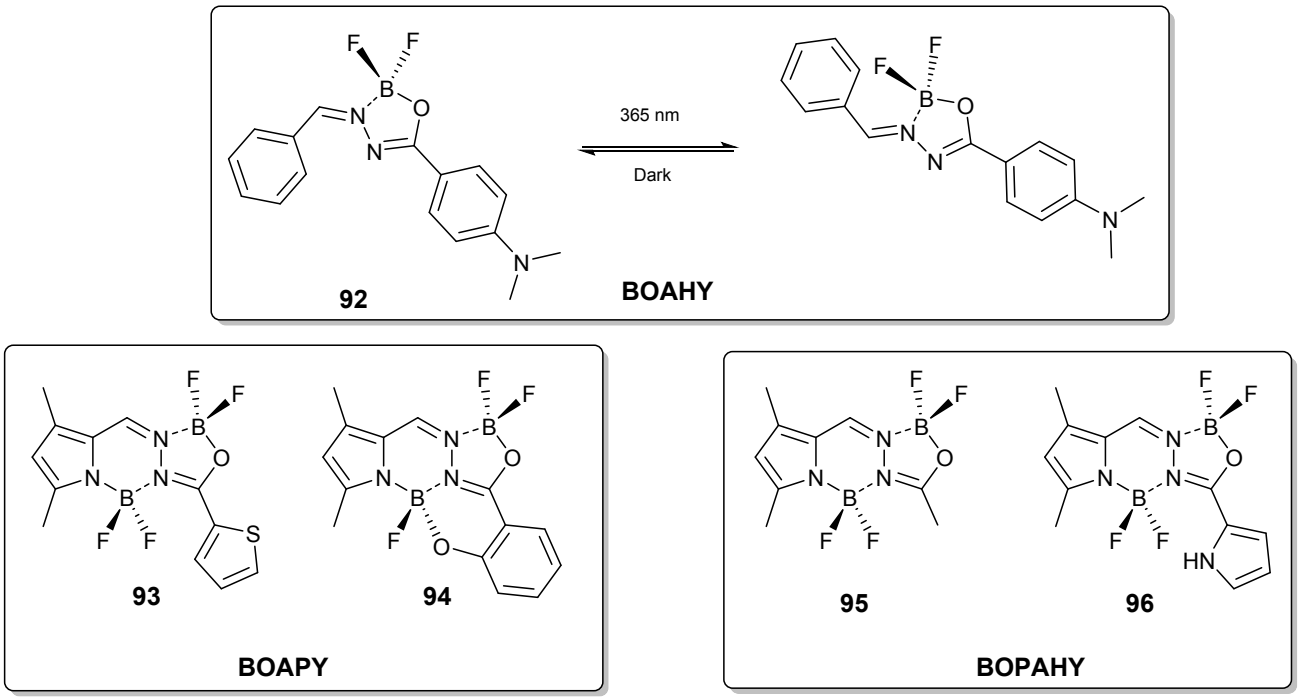

Scheme 21.

The addition of the second BF_2 coordination site gave the rise of BOAPY (bis-BOron difluoride-coordinated PYrrolyl−Acylhydrazone) family fluorophores **93** and **94** (Scheme 21). BOAPYs have increased fluorescence both in solution and the solid state (Φ_F of up to 0.88 and 0.64, respectively).[122] Interestingly, BOAPY can form both BF_2 and B-O types (**93**) and B-O types (BOAPY **94**) of coordination depending on their structure. Dehaen's group has recently reported similar to BOAPY bis(difluoroboron) pyrrole acylhydrazones (BOPAHY) structures **95** and **96**.[123] Authors point out that while BODIPY is a polymethine dye, the BOPAHYs can be considered heavily substituted polyenes, and, comparing to tetramethyl-substituted BODIPY, the main absorption peak of **95** is significantly blue-shifted, from 500 to 375 nm in acetonitrile, while maximum emission occurs at 388 nm. Replacing the methyl group at the 5-position with thiophene, furan, or pyrrole (**96**), leads, in all cases, to a red shift in absorption and emission maxima to 409-428 nm and 439-536 nm regions, respectively, with fluorescence quantum yields up to 0.76 in acetonitrile.

3. Conclusions and outlook. The prominent optical and especially fluorescent properties of the BODIPYs sparked scientific curiosity in the academic and currently industrial world. Not surprisingly, in pursuit of new chromophores with fine-tuned optical and fluorescence responses, BODIPY core chemistry was extended to aza-BODIPY and later on to BOPHY

chromophores. The numerous modifications of the aza-BODIPY's and BOPHY's structural motifs resulted is several new platforms discovered just in the last five years. There is no doubt that the rational design of the new chromophores based on the systems discussed in this review will continue in the future to address technological needs of society. Thus, we are looking forward with a great enthusiasm and excitement toward the novel applications of the newly discovered and future chromophoric systems.

ORCID

Liliya I. Shamova: 0000-0002-5320-0175

Yuriy V. Zatsikha: 0000-0002-9770-7007

Victor N. Nemykin: 0000-0003-4345-0848

Notes

The authors declare no competing financial interests.

ACKNOWLEDGMENT

Generous support from the University of Manitoba, NSF, and the University of Tennessee to VN is greatly appreciated.

LIST OF ABBREVIATIONS

BODIPY	4,4'-difluoro-4-bora-3a,4a-diaza-*s*-indacene
Aza-BODIPY	4,4'-difluoro-4-bora-3a,4a,8-triaza-*s*-indacene
BOPHY	bis(difluoroboron)1,2-bis((1H-pyrrol-2- yl)methylene)hydrazine
MB-DIPY	"Manitoba – dipyrromethene"
BOIMPY 1	boron complexes of iminopyrrolide ligands

BOIMPY 2	(bis(borondifluoride)-8-imidazodipyrromethene)
BOPPY	double boron complexes of pyrrole- N-heteroarene derivative
BOPYPY	5,6,5,6-tetracyclic pyrazine/pyrrole-fused unsymmetric bis(BF_2) fluorescent dyes
BOAHY	difuoroboronate anchored acylhydrazones
BOAPY	bis-boron difluoride-coordinated pyrrolyl−acylhydrazone

References

1 R. A. Baglia, J. P. T. Zaragoza and D. P. Goldberg, *Chem. Rev.*, 2017, **117**, 13320–13352.

2 E. Sitte and M. O. Senge, *European J. Org. Chem.*, 2020, 3171–3191.

3 J. P. T. Zaragoza and D. P. Goldberg, *RSC Met.*, 2019, **13**, 3–36.

4 A. R. Battersby and E. McDonald, *Acc. Chem. Res.*, 1979, **12**, 14–22.

5 V. N. Nemykin, S. V. Dudkin, F. Dumoulin, C. Hirel, A. G. Gürek and V. Ahsen, *ARKIVOC*, 2014, (*i*), 142–204.

6 M. Urbani, G. De La Torre, M. K. Nazeeruddin and T. Torres, *Chem. Soc. Rev.*, 2019, **48**, 2738–2766.

7 M. Urbani, M. E. Ragoussi, M. K. Nazeeruddin and T. Torres, *Coord. Chem. Rev.*, 2019, **381**, 1–64.

8 V. E. Pushkarev, L. G. Tomilova and V. N. Nemykin, *Coord. Chem. Rev.*, 2016, **319**, 110–179.

9 Y. Mulyana and K. Ishii, *Dalton Trans.*, 2014, **43**, 17596–17605.

10 E. A. Lukyanets and V. N. Nemykin, *J. Porphyrins Phthalocyanines*, 2010, **14**, 1–40.

11 S. Osati, H. Ali and J. E. Van Lier, *J. Porphyrins Phthalocyanines*, 2016, **20**, 61–75.

12 W. Zhang, A. Ahmed, H. Cong, S. Wang, Y. Shen and B. Yu, *Dyes Pigments*, 2021, **185**, 108937.

13 Y. Chiba, T. Nakamura, R. Matsuoka and T. Nabeshima, *Synlett*, 2020, **31**, 1663–1681.

14 M. Poddar and R. Misra, *Coord. Chem. Rev.*, 2020, **421**, 213462.

15 J. Wang, Q. Gong, L. Wang, E. Hao and L. Jiao, *J. Porphyrins Phthalocyanines*, 2020, **24**,

603–635.

16 J. Wang, N. Boens, L. Jiao and E. Hao, *Org. Biomol. Chem.*, 2020, **18**, 4135–4156.

17 J. Zhang, N. Wang, X. Ji, Y. Tao, J. Wang and W. Zhao, *Chem. Eur. J.*, 2020, **26**, 4172–4192.

18 Z. Shi, X. Han, W. Hu, H. Bai, B. Peng, L. Ji, Q. Fan, L. Li and W. Huang, *Chem. Soc. Rev.*, 2020, **49**, 7533–7567.

19 G. Kalot, A. Godard, B. Busser, J. Pliquett, M. Broekgaarden, V. Motto-Ros, K. D. Wegner, U. Resch-Genger, U. Köster, F. Denat, J. L. Coll, E. Bodio, C. Goze and L. Sancey, *Cells*, 2020, **9**, 1953.

20 D. Chen, Z. Zhong, Q. Ma, J. Shao, W. Huang, X. Dong and X. Dong, *ACS Appl. Mater. Interfaces*, 2020, **12**, 26914–26925.

21 G. Qian and Z. Y. Wang, *Chem Asian J*, 2010, **5**, 1006–1029.

22 Y. Ge and D. F. O'Shea, *Chem. Soc. Rev.*, 2016, **45**, 3846–3864.

23 a) M. A. T. Rogers, *J. Chem. Soc.*, 1943, 590–596; b) M. A. T. Rogers, *Nature*, 1943, **151**, 504; c) W. H. Davies and M. A. T. Rogers, *J. Chem. Soc.*, 1944, 126–131.

24 A. Gorman, J. Killoran, C. O'Shea, T. Kenna, W. M. Gallagher and D. F. O'Shea, *J. Am. Chem. Soc.*, 2004, **126**, 10619–10631.

25 M. J. Hall, S. O. McDonnell, J. Killoran and D. F. O'Shea, *J. Org. Chem.*, 2005, **70**, 5571–5578.

26 N. O. Didukh, Y. V. Zatsikha, G. T. Rohde, T. S. Blesener, V. P. Yakubovskyi, Y. P. Kovtun and V. N. Nemykin, *Chem. Commun.*, 2016, **52**, 11563–11566.

27 C. J. Ziegler, K. Chanawanno, A. Hasheminsasab, Y. V. Zatsikha, E. Maligaspe and V. N. Nemykin, *Inorg. Chem.*, 2014, **53**, 4751–4755.

28 Y. V. Zatsikha, C. D. Holstrom, K. Chanawanno, A. J. Osinski, C. J. Ziegler and V. N. Nemykin, *Inorg. Chem.*, 2017, **56**, 991–1000.

29 Y. V. Zatsikha, T. S. Blesener, P. C. Goff, A. T. Healy, R. K. Swedin, D. E. Herbert, G. T. Rohde, K. Chanawanno, C. J. Ziegler, R. V. Belosludov, D. A. Blank and V. N. Nemykin, *J. Phys. Chem. C*, 2018, **122**, 27893–27916.

30 L. Gao, W. Senevirathna and G. Sauvé, *Org. Lett.*, 2011, **13**, 5354–5357.

31 L. Gao, N. Deligonul and T. G. Gray, *Inorg. Chem.*, 2012, **51**, 7682–7688.

32 X. D. Jiang, D. Xi, B. Le Guennic, J. Guan, D. Jacquemin, J. Guan and L. J. Xiao, *Tetrahedron*, 2015, **71**, 7676–7680.

33 Y. Gawale, N. Adarsh, S. K. Kalva, J. Joseph, M. Pramanik, D. Ramaiah and N. Sekar,

Chem. Eur. J., 2017, **23**, 6570–6578.

34 X. D. Jiang, L. Jia, Y. Su, C. Li, C. Sun and L. Xiao, *Tetrahedron*, 2019, **75**, 4556–4560.

35 H. Ş. Çınar, Ş. Özçelik, K. Kaya, Ö. D. Kutlu, A. Erdoğmuş and A. Gül, *J. Mol. Struct.*, 2020, **1200**, 127108.

36 A. Y. Kritskaya, M. B. Berezin, E. V. Antina and A. I. Vyugin, *J. Fluorescence*, 2019, **29**, 911–920.

37 A. Kamkaew and K. Burgess, *Chem. Commun.*, 2015, **51**, 10664–10667.

38 W. Shi, P. Lo and D. K. P. Ng, *Dyes Pigments*, 2018, **154**, 314–319.

39 S. Pascal, Q. Bellier, S. David, P. A. Bouit, S. H. Chi, N. S. Makarov, B. Le Guennic, S. Chibani, G. Berginc, P. Feneyrou, D. Jacquemin, J. W. Perry, O. Maury and C. Andraud, *J. Phys. Chem. C*, 2019, **123**, 23661–23673.

40 S. Osati, H. Ali, B. Guerin and J. E. Van Lier, *Steroids*, 2017, **123**, 27–36.

41 C. Wang, C. Daddario, S. Pejić and G. Sauvé, *Eur. J. Org. Chem.*, 2020, 714–722.

42 A. Koch, S. Kumar and M. Ravikanth, *Tetrahedron*, 2017, **73**, 1459–1465.

43 S. Kumar, T. K. Khan and M. Ravikanth, *Tetrahedron*, 2015, **71**, 7608–7613.

44 W. Sheng, Y. Zheng, Q. Wu, Y. Wu, C. Yu, L. Jiao, E. Hao, J. Wang and J. Pei, *Org. Lett*., 2017, **19**, 2893−2896.

45 W. Sheng, Y. Wu, C. Yu, P. Bobadova-Parvanova, E. Hao and L. Jiao, *Org. Lett.*, 2018, **20**, 2620–2623.

46 W. Sheng, Y. Q. Zheng, Q. Wu, K. Chen, M. Li, L. Jiao, E. Hao, J. Y. Wang and J. Pei, *Sci. China Chem.*, 2020, **63**, 1240–1245.

47 L. Jiao, C. Yu, J. Li, Z. Wang, M. Wu and E. Hao, *J. Org. Chem.*, 2009, **74**, 7525–7528.

48 J. Wang, Y. Wu, W. Sheng, C. Yu, Y. Wei, E. Hao and L. Jiao, *ACS Omega*, 2017, **2**, 2568–2576.

49 A. Palma, M. Tasior, D. O. Frimannsson, T. T. Vu, R. Méallet-Renault and D. F. O'Shea, *Org. Lett.*, 2009, **11**, 3638–3641.

50 R. K. Swedin, Y. V. Zatsikha, A. T. Healy, N. O. Didukh, T. S. Blesener, M. Fathi-Rasekh, T. Wang, A. J. King, V. N. Nemykin and D. A. Blank, *J. Phys. Chem. Lett.*, 2019, **10**, 1828–1832.

51 A. Loudet, R. Bandichhor, K. Burgess, A. Palma, S. O. Mcdonnell, M. J. Hall and D. F. O. Shea, *Org. Lett.*, 2008, **10**, 4771–4774.

52 Y. Kubo, T. Shimada, K. Maeda and Y. Hashimoto, *New J. Chem.*, 2020, **44**, 29–37.

53 X. D. Jiang, Y. Fu, T. Zhang and W. Zhao, *Tetrahedron Lett.*, 2012, **53**, 5703–5706.

54 S. A. Berhe, M. T. Rodriguez, E. Park, V. N. Nesterov, H. Pan and W. J. Youngblood, *Inorg. Chem.*, 2014, **53**, 2346–2348.

55 R. M. Diaz-Rodriguez, L. Burke, K. N. Robertson and A. Thompson, *Org. Biomol. Chem.*, 2020, **18**, 2139–2147.

56 M. Wang, G. Zhang, N. E. M. Kaufman, P. Bobadova-Parvanova, F. R. Fronczek, K. M. Smith and M. G. H. Vicente, *Eur. J. Org. Chem.*, 2020, 971–977.

57 O. Florès, J. Pliquett, L. Abad Galan, R. Lescure, F. Denat, O. Maury, A. Pallier, P. S. Bellaye, B. Collin, S. Même, C. S. Bonnet, E. Bodio and C. Goze, *Inorg. Chem.*, 2020, **59**, 1306–1314.

58 J. Pliquett, A. Dubois, C. Racoeur, N. Mabrouk, S. Amor, R. Lescure, A. Bettaïeb, B. Collin, C. Bernhard, F. Denat, P. S. Bellaye, C. Paul, E. Bodio and C. Goze, *Bioconjug. Chem.*, 2019, **30**, 1061–1066.

59 V. F. Donyagina, S. Shimizu, N. Kobayashi and E. A. Lukyanets, *Tetrahedron Lett.*, 2008, **49**, 6152–6154.

60 A. Dyes, R. Gresser, M. Hummert, H. Hartmann, K. Leo and M. Riede, *Chem. Eur. J.*, 2011, **17**, 2939–2947.

61 L. Zhang, L. Zhao, K. Wang and J. Jiang, *Dyes Pigments*, 2016, **134**, 427–433.

62 B. Zou, H. Liu, J. Mack, S. Wang, J. Tian, H. Lu, Z. Li and Z. Shen, *RSC Adv.*, 2014, **4**, 53864–53869.

63 W. Zheng, B. Wang, C. Li, J. Zhang and C. Wan, *Angew. Chem. Int. Ed.*, 2015, **54**, 9070–9074.

64 G. R. Mckeown, J. G. Manion, A. J. Lough and D. S. Seferos, *Chem. Commun.*, 2018, **54**, 8893–8896.

65 E. Maligaspe, T. J. Pundsack, L. M. Albert, Y. V. Zatsikha, P. V. Solntsev, D. A. Blank and V. N. Nemykin, *Inorg. Chem.*, 2015, **54**, 4167–4174.

66 M. Lorenz-Rothe, K. S. Schellhammer, T. Jägeler-Hoheisel, R. Meerheim, S. Kraner, M. P. Hein, C. Schünemann, M. L. Tietze, M. Hummert, F. Ortmann, G. Cuniberti, C. Körner and K. Leo, *Adv. Electron. Mater.*, 2016, **2**, 1–11.

67 L. A. Crandall, H. M. Rhoda, V. N. Nemykin and C. J. Ziegler, *New J. Chem.*, 2016, **40**, 5675–5678.

68 L. A. Crandall, C. A. Bogdanowicz, A. Hasheminasab, K. Chanawanno, R. S. Herrick and C. J. Ziegler, *Inorg. Chem.*, 2016, 3209–3211.

69 B. R. Schrage, V. N. Nemykin and C. J. Ziegler, *Chem. Commun.*, 2020, **56**, 6628–6631.

70 A. Díaz-Moscoso, E. Emond, D. L. Hughes, G. J. Tizzard, S. J. Coles and A. N. Cammidge, *J. Org. Chem.*, 2014, **79**, 8932–8936.

71 Y. V Zatsikha, L. I. Shamova, T. S. Blesener, I. A. Kuzmin, Y. V Germanov, D. E. Herbert and V. N. Nemykin, *J. Org. Chem.*, 2019, **84**, 14540–14557.

72 Y. V. Zatsikha, L. I. Shamova, T. S. Blesener, D. E. Herbert and V. N. Nemykin, *Dalton Trans.*, 2020, **49**, 5034–5038.

73 Y. V. Zatsikha, L. I. Shamova, J. W. Schaffner, A. T. Healy, T. S. Blesener, G. Cohen, B. Wozniak, D. A. Blank and V. N. Nemykin, *ACS Omega*, 2020, **5**, 28656–28662.

74 Y. V. Zatsikha, E. Maligaspe, A. A. Purchel, N. O. Didukh, Y. Wang, Y. P. Kovtun, D. A. Blank and V. N. Nemykin, *Inorg. Chem.*, 2015, **54**, 7915–7928.

75 A. J. Osinski, T. Blesener, A. Hasheminasab, C. Holstrom, V. N. Nemykin, R. S. Herrick and C. J. Ziegler, *Inorg. Chem.*, 2016, **55**, 12527–12530.

76 W. Sheng, F. Chang, Q. Wu, E. Hao, L. Jiao, J. Y. Wang and J. Pei, *Org. Lett.*, 2020, **22**, 185–189.

77 S. Shimizu, *Chem. Commun.*, 2019, **55**, 8722–8743.

78 M. Tamada, T. Iino, Y. Wang, M. Ide, A. Saeki, H. Furuta, N. Kobayashi and S. Shimizu, *Tetrahedron Lett.*, 2017, **58**, 3151–3154.

79 S. Shimizu, T. Iino, Y. Araki and N. Kobayashi, *Chem. Commun.*, 2013, **49**, 1621–1623.

80 Y. Kage, H. Karasaki, S. Mori, H. Furuta and S. Shimizu, *ChemPlusChem*, 2019, **84**, 1648–1652.

81 R. Feng, N. Sato, T. Yasuda, H. Furuta and S. Shimizu, *Chem. Commun.*, 2020, **56**, 2975–2978.

82 I. S. Tamgho, A. Hasheminasab, J. T. Engle, V. N. Nemykin and C. J. Ziegler, *J. Am. Chem. Soc.*, 2014, **136**, 5623–5626.

83 C. Yu, L. Jiao, P. Zhang, Z. Feng, C. Cheng, Y. Wei, X. Mu and E. Hao, *Org. Lett.*, 2014, **16**, 3048–3051.

84 L. Wang, I. S. Tamgho, L.A. Crandall, J.J. Rack, C.J. Ziegler, *Phys. Chem. Chem. Phys.,* 2015, **17**, 2349–2351.

85 A. P. Demchenko, *Methods Appl. Fluorescence*, 2020, **8**, 002001.

86 R. Sola-Llano, J. Jiménez, E. Avellanal-Zaballa, M. Johnson, T. A. Cabreros, F. Moreno, B. L. Maroto, G. Muller, J. Bañuelos, L. Cerdán, I. García-Moreno and S. de la Moya, *Dyes Pigments*, 2019, **170**, 107662.

87 S. Boodts, J. Hofkens and W. Dehaen, *Dyes Pigments*, 2017, **142**, 249–254.

88 X. Lv, T. Li, Q. Wu, C. Yu, L. Jiao and E. Hao, *J. Org. Chem.*, 2018, **83**, 1134–1145.

89 T. F. Cui, J. Zhang, X. D. Jiang, Y. J. Su, C. L. Sun and J. L. Zhao, *Chinese Chem. Lett.*, 2016, **27**, 190–194.

90 R. R. Mallah, D. R. Mohbiya, M. C. Sreenath, S. Chitrambalam, I. H. Joe and N. Sekar, *Spectrochim. Acta A*, 2019, **215**, 122–129.

91 X. Li, G. Ji and Y. A. Son, *Dyes Pigments*, 2016, **124**, 232–240.

92 Q. Huaulmé, A. Mirloup, P. Retailleau and R. Ziessel, *Org. Lett.*, 2015, **17**, 2246–2249.

93 C. G. López-Calixto, M. Liras, V. A. de la Peña O'Shea and R. Pérez-Ruiz, *Appl. Catal. B Environ.*, 2018, **237**, 18–23.

94 C. Zhang and J. Zhao, *J. Mater. Chem. C*, 2016, **4**, 1623–1632.

95 C. G. López-Calixto, S. Cabrera, R. Pérez-Ruiz, M. Barawi, J. Alemán, V. A. de la Peña O'Shea and M. Liras, *Appl. Catal. B Environ.*, 2019, **258**, 117933.

96 C. G. López-Calixto, M. Barawi, M. Gomez-Mendoza, F. E. Oropeza, F. Fresno, M. Liras, V. A. De La Penã O'Shea and V. A. de la Peña O'Shea, *ACS Catal.*, 2020, **10**, 9804–9812.

97 L. Jiang, H. Gao, L. Gai and Z. Shen, *New J. Chem.*, 2018, **42**, 8271–8275.

98 A. Mirloup, Q. Huaulmé, N. Leclerc, P. Lévêque, T. Heiser, P. Retailleau and R. Ziessel, *Chem. Commun.*, 2015, **51**, 14742–14745.

99 H. M. Rhoda, K. Chanawanno, A. J. King, Y. V. Zatsikha, C. J. Ziegler and V. N. Nemykin, *Chem. Eur. J.*, 2015, **21**, 18043–18046.

100 X. D. Jiang, Y. Su, S. Yue, C. Li, H. Yu, H. Zhang, C. L. Sun and L. J. Xiao, *RSC Adv.*, 2015, **5**, 16735–16739.

101 D. Cheng, X. Liu, Y. Xie, H. Lv, Z. Wang, H. Yang, A. Han, X. Yang and L. Zang, *Sensors*, 2017, **17**, 2517.

102 C. He, H. Zhou, N. Yang, N. Niu, E. Hussain, Y. Li and C. Yu, *New J. Chem.*, 2018, **42**, 2520–2525.

103 O.J. Woodford, R. Ziessel, A. Harriman, *ChemPhotoChem*, 2018, **2**, 1046–1054.

104 O.J. Woodford, P. Stachelek, R. Ziessel, N. Algoazy, J.G. Knight, A. Harriman, *New J. Chem.*, 2018, **42**, 4835–4842.

105 O.J. Woodford, R. Ziessel, A. Harriman, C. Wills, A.A. Alsimaree, J.G. Knight, *Spectrochim. Acta A Mol. Biomol. Spectr.*, 2019, **208**, 57–64.

106 Y. V. Zatsikha, D. B. Nemez, R. L. Davis, S. Singh, D. E. Herbert, A. J. King, C. J.

Ziegler and V. N. Nemykin, *Chem. Eur. J.*, 2017, **23**, 14786–14796.

107 Y. Li, H. Zhou, S. Yin, H. Jiang, N. Niu, H. Huang, S. A. Shahzad and C. Yu, *Sensors Actuators, B Chem.*, 2016, **235**, 33–38.

108 L. Gai, J. Xu, Y. Wu, H. Lu and Z. Shen, *New J. Chem.*, 2016, **40**, 5752–5757.

109 F. Meng, Y. Sheng, F. Li, C. Zhu, Y. Quan and Y. Cheng, *RSC Adv.*, 2017, **7**, 15851–15856.

110 J. Wang, Q. Wu, C. Yu, Y. Wei, X. Mu, E. Hao and L. Jiao, *J. Org. Chem.*, 2016, **81**, 11316–11323.

111 L. Zhou, D. Xu, H. Gao, C. Zhang, F. Ni, W. Zhao, D. Cheng, X. Liu and A. Han, *J. Org. Chem.*, 2016, **81**, 7439–7447.

112 B. Lee, B. G. Park, W. Cho, H. Y. Lee, A. Olasz, C. H. Chen, S. B. Park and D. Lee, *Chem. Eur. J.*, 2016, **22**, 17321–17328.

113 A. I. Rodrigues, P. Krishnamoorthy, C. S. B. Gomes, N. Carmona, R. E. Di Paolo, P. Pander, J. Pina, J. Sérgio Seixas de Melo, F. B. Dias, M. J. Calhorda, A. L. Maçanita, J. Morgado and P. T. Gomes, *Dalton Trans.*, 2020, **49**, 10185–10202.

114 L. J. Patalag, P. G. Jones and D. B. Werz, *Angew. Chem. Int. Ed.*, 2016, **55**, 13340–13344.

115 B. C. De Simone, G. Mazzone, N. Russo, E. Sicilia and M. Toscano, *Phys. Chem. Chem. Phys.*, 2018, **20**, 2656–2661.

116 B. Le Guennic, G. Scalmani, M. J. Frisch, A. D. Laurent and D. Jacquemin, *Phys. Chem. Chem. Phys.*, 2017, **19**, 10554–10561.

117 L. J. Patalag, P. G. Jones and D. B. Werz, *Chem. Eur. J.*, 2017, **23**, 15903–15907.

118 L. J. Patalag, M. Loch, P. G. Jones and D. B. Werz, *J. Org. Chem.*, 2019, **84**, 7804–7814.

119 C. Yu, Z. Huang, X. Wang, W. Miao, Q. Wu, W. Y. Wong, E. Hao, Y. Xiao and L. Jiao, *Org. Lett.*, 2018, **20**, 4462–4466.

120 X. Jiang, S. Yue, K. Chen, Z. Shao, C. Li, Y. Su and J. Zhao, *Chin. Chem. Lett.*, 2019, **30**, 2271–2273.

121 C. Yu, E. Hao, X. Fang, Q. Wu, L. Wang, J. Li, L. Xu, L. Jiao and W. Y. Wong, *J. Mater. Chem. C*, 2019, **7**, 3269–3277.

122 C. Yu, X. Fang, Q. Wu, L. Jiao, L. Sun, Z. Li, P. K. So, W. Y. Wong and E. Hao, *Org. Lett.*, 2020, **22**, 4588–4592.

123 S. Pookkandam Parambil, F. de Jong, K. Veys, J. Huang, S. P. Veettil, D. Verhaeghe, L. Van Meervelt, D. Escudero, M. Van der Auweraer and W. Dehaen, *Chem. Commun.*, 2020, **56**, 5791–5794.

Graphical abstract: